CERAMIDE-INDUCED ALTERNATIVE TRANSLOCATION

OF TM4SF20

APPROVED BY SUPERVISORY COMMITTEE

Jin Ye, Ph.D.

Julie Pfeiffer, Ph.D.

Steve McKnight, Ph.D

Jeffrey Kahn, M.D.

Deepak Nijhawan, M.D., Ph.D

This thesis is dedicated to my parents:

for supporting me in all that I do.

Even when I worry them to no end.

CERAMIDE-INDUCED ALTERNATIVE TRANSLOCATION OF TM4SF20

by

CHING EN LEE

DISSERTATION / THESIS

Presented to the Faculty of the Graduate School of Biomedical Sciences

The University of Texas Southwestern Medical Center at Dallas

In Partial Fulfillment of the Requirements

For the Degree of

DOCTOR OF PHILOSOPHY

The University of Texas Southwestern Medical Center at Dallas

Dallas, Texas

December, 2015

Acknowledgements

I would like to first thank Dr. Jin Ye for mentoring me, without his mentorship my training would have remained incomplete. In Jin's laboratory, I have learned a great deal about how to methodically tackle scientific problems, even if I do remain incredibly pessimistic about every bit of data I see. I also need to thank Dr. Bray Denard for his guidance over the years, as his work was the starting line for what Dr. Qiuyue Chen, and then I, studied. Special thanks also goes to Dr. Qiuyue Chen, whose work is the foundation for my own thesis work.

I want to acknowledge the technicians and head of the Tissue Culture Core Lisa Beatty and all the technicians over the years. Similarly, without the technical aid of Jeff Cormier, Lisa Donelly, and past laboratory member Saada Abdalla; research would have been much slower. Ruth Gordillo (UT Southwestern Metabolic Phenotyping Core) for mass spectrometry quantitation of sphingolipids in biological samples and Shimadzu Scientific Instruments for the collaborative effort. None of this would be possible without the support of Dr. Michael Brown and Dr. Joseph Goldstein for creating a supportive and friendly department.

I thank my committee members Dr. Julie Pfeiffer, Dr. Steve McKnight, Dr. Deepak Nijhawan, and Dr. Jeffrey Kahn for their valuable time and advice.

To all of the past and present members of the Ye lab, Drs. Hongbing Yao, Bray Denard, Hyeonwoo Kim, Qiuyue Chen, Jinyong Kim, Sungwon Han, Glenn Simmons, and our lab manager, JungYeon Kim; thank you for making the lab a pleasant place to be despite our lack of windows.

CERAMIDE-INDUCED ALTERNATIVE TRANSLOCATION

OF TM4SF20

Publication No. _____

Ching En Lee, Ph.D.

The University of Texas Southwestern Medical Center at Dallas, 2015

Supervising Professor: Jin Ye, Ph.D.

The polytopic membrane protein TM4SF20 (transmembrane 4 L6 family 20) is a protein containing four transmembrane helices that inhibits the Regulated Intramembrane Proteolysis (RIP) of the transcriptional factor CREB3L1 (cAMP response element binding protein 3-like 1), a transcription factor synthesized as a membrane-bound precursor. CREB3L1 RIP is induced by several stimuli: ER stress, viral infections, the chemotherapeutic drug, doxorubicin, and the sphingolipid, ceramide. Additionally, TGF-β (transforming growth factor-β), a cytokine known to stimulate collagen production,

induces the proteolytic activation of CREB3L1 in human A549 cells through inhibition of TM4SF20 expression, which normally inhibits RIP of CREB3L1. We also find that the TM4SF20 regulation of CREB3L1 RIP is regulated by ceramide. In this study we find that ceramide can regulate the ability of first transmembrane domain of TM4SF20 to determine its orientation in the membrane. Under normal conditions, TM4SF20 is synthesized as a protein that inhibits the cleavage of CREB3L1 when TRAM2 (translocation associated membrane protein 2) is associated with the ER translocon. Excess ceramide dissociates TRAM2 from the ER translocon such that the N-terminus of TM4SF20 can no longer be forced by the first transmembrane domain to function as a signal peptide. Under excess ceramide conditions, TM4SF20 adopts a completely opposite topology and allows the cleavage of CREB3L1 to proceed. We have designated this novel mechanism for transmembrane protein regulation as "alternative translocation."

TABLE OF CONTENTS

PRIOR PUBLICATIONS

Chen Q., **Lee C.**, Denard B., Ye J. (2014) Sustained Induction of Collagen Synthesis by TGF-b Requires Regulated Intramembrane Proteolysis of CREB3L1. PLoS ONE 9(10): e108528. doi:10.1371/journal.pone.0108528

Hondorp E.R., Hou S., Hause L., Gera K. , **Lee C.**, and McIver K.S. (2013) PTS phosphorylation of Mga modulates regulon expression and virulence in the group A streptococcus, Molecular Microbiology, 88(6):1176-1193.

Denard B., **Lee C.**, Ye J. 2012. Doxorubicin blocks proliferation of cancer cells through proteolytic activation of CREB3L1. eLife 1:e00090. doi: 10.7554/elife.00090.

LIST OF FIGURES

LIST OF ABBREVIATIONS

ATF6 – Activating Transcription Factor 6

BMP2 – Bone Morphogenetic Protein 2

CREB3L1– Cyclic AMP-Responsive Element-Binding Protein 3-Like Protein 1

Endo H – Endoglycosidase H

ER – Endoplasmic Reticulum

ERK – Extracellular Signal-regulated Kinase

GFP – Green Fluorescent Protein

OASIS – Old-Astrocyte Specifically Induced Substance

AP – Placental Alkaline Phosphatase

PNGase F – Peptide-N-Glycosidase F

RIP– Regulated Intramembrane Proteolysis

RT-QPCR – Real time- Quantitative Polymerase Chain Reaction

S1P – Site-1 Protease

S2P – Site-2 Protease

SMase – Sphingomyelinase

SPCS3 – Signal Peptidase Complex Subunit 3

SPT – Serine Palmitoyl Transferase

SREBPs – Sterol Regulatory Element Binding Proteins

SRP – Signal Recognition Particle

TGF-β – Transforming Growth Factor Beta

TM4SF20 – Transmembrane 4 L Six Family Member 20

TRAM1 –Translocation Associated Membrane Protein 1

TRAM1L1 –Translocation Associated Membrane 1-like Protein 1

TRAM2 – Translocation Associated Membrane Protein 2

CHAPTER ONE
Introduction

Regulated Intramembrane Proteolysis

Regulated Intramembrane Proteolysis (RIP) allows cells to transmit signals from the endoplasmic reticulum (ER) to the nucleus. The most well-characterized RIP-dependent signaling pathway is the proteolytic activation of the sterol regulatory element binding proteins (SREBPs). SREBPs are transmembrane proteins located in the ER that respond to the level of sterols in the cells, and were characterized in the context of their response to cholesterol (Ye et al., 2000a). When cells have a high amount of sterols, SREBPs reside in the ER, but upon sterol depletion, SREBPs translocate from the ER to the Golgi. In the Golgi, SERBP are sequentially cleaved by Site-1 Protease (S1P) and Site-2 Protease (S2P) (DeBose-Boyd et al., 1999; Sakai et al., 1996). These proteolytic cleavages of SREBPs result in the release of the N-terminal portion of SREBPs from the membrane, allowing them to enter the nucleus to activate the transcription of genes involved in cholesterol synthesis (Ye and DeBose-Boyd, 2011). The highly regulated process of RIP involves proteins other than SREBP, S1P, and S2P. Two other transmembrane proteins regulating SREBP RIP: Scap and Insig, which function to escort SREBP to the Golgi for protelytic activation or retain SREBP in the ER in its inactive form, respectively. Another RIP substrate, the activation transcription factor 6 (ATF6), is

also retained in the ER through interaction with its regulatory inhibitor, BiP (Shen et al., 2002). ER stress leads to the dissociation of BiP from ATF6, permitting the transport of ATF6 from the ER to Golgi to undergo proteolytic activation by S1P and S2P (Shen et al., 2002; Ye et al., 2000b).

The Transcription Factor CREB3L1

The transcriptional factor cAMP-Responsive Element-Binding Protein 3-Like Protein 1 (CREB3L1) was originally identified in astrocytes and named Old-Astrocyte Specifically Induced Substance (OASIS) (Honma et al, 1999). The high expression of CREB3L1 mRNA in developing mouse osteoblasts in addition to the decreased bone density seen in CREB3L1 genetic knock-out mice suggests that the membrane-bound transcription factor has a role in bone development (Nikaido et al., 2001; Murakami et al., 2009).

CREB3L1 is part of a family of transcription factors synthesized as transmembrane precursors (Omori et al., 2002), containing recognition sequences for S1P (Hua et al., 1996) and S2P (Ye et al., 2000a). As a membrane-bound transcription factor, CREB3L1 has been shown to undergo RIP in response to ER stress such as the treatment of cells by tunicamycin, thapsigargin, and by viral infection (Murakami et al, 2006; Denard et al., 2011). Another stimuli demonstrated to induce CREB3L1 RIP is Bone Morphogenetic Protein 2 (BMP2) in osteoblasts which activates the transcription of type I collagen (Murakami, 2009). CREB3L1 was also found to respond to the chemotherapeutic drug, doxorubicin, which causes CREB3L1 RIP (Denard et al, 2012). Doxorubicin was found to induce the *de novo* synthesis of ceramide, and it is the

accumulation of ceramide in the ER which triggers CREB3L1 RIP in response to doxorubicin (Denard et al., 2012). This proteolytic cleavage of CREB3L1 releases the N-terminal transcription factor domain from the membrane, allowing it to enter the nucleus and activate transcription of genes that inhibit cell cycle progression and stimulate assembly of collagen-containing extracellular matrices (Denard et al., 2011; Murakami et al., 2009).

Ceramide is a sphingolipid known to have signaling activity, and has been shown to inhibit cell proliferation (Morad and Cabot, 2013). It is a composed of sphingosine, an 18-carbon unsaturated amino alcohol hydrocarbon chain, linked by an amide to a fatty acid of varying chain lengths and degrees of saturation (Morad and Cabot, 2013). Ceramide can be produced by the cell through three pathways. This sphingolipid can be generated by the hydrolysis of sphingomyelin on the plasma membrane by sphingomyelinase (SMase) to produce phosphocholine and ceramide. Ceramide is also synthesized *de novo* by serine palmitoyl transferase (SPT) and ceramide synthases in the ER (Hannun and Obeid, 2008). Lastly, ceramide can be generated is through the ceramide salvage pathway in which ceramide synthases recycle long-chain sphingoidlipid bases to form ceramide as an end product back in the ER (Kitatani et al, 2008). The location of ceramide in the ER is of particular interest as the sphingolipid is expected to be in the correct cellular compartment to be able to interact with the membrane-bound form of CREB3L1.

Another stimuli of CREB3L1 RIP is the transforming-growth factor ß (TGF- ß). TGF-ß is a cytokine homologous to BMP2, previously reported to induce the RIP of

CREB3L1, and like BMP2, TGF-ß also activates collagen synthesis (Murakami et al., 2009; Verrechia and Mauviel, 2007). TGF-ß was identified to induce the proteolytic activation of CREB3L1 in human A549 cells. Furthermore, it was demonstrated that the RIP of CREB3L1 is specifically required for TGF-ß to chronically induce transcription of genes involved in the assembly of collagen extracellular matrix (Chen et al., 2014).

When considering the regulation of CREB3L1 in the context of previously well-characterized examples of RIP, such as SREBP and ATF6, it is clear that there ought to be other regulatory proteins in the CREB3L1 RIP dependent signaling pathway. Both SREBPs and ATF6 have additional regulatory transmembrane proteins that regulate RIP, and like the RIP substrates, a regulatory transmembrane protein for CREB3L1 RIP was identified.

TM4SF20 is a Regulator of CREB3L1 RIP

In a previous study, protein transmembrane 4 L6 family member 20 (TM4SF20) was identified as an inhibitory regulatory protein of CREB3L1 RIP (Chen et al., 2014). TM4SF20 is a polytopic membrane protein that belongs to a family of proteins containing four transmembrane domains (Wright et al., 2000). This transmembrane protein may be involved language development in humans, as the deletion of exon 3 of TM4SF20 is associated with early childhood communication disorders (Wiszniewski et al., 2013). TGF-β was found to induce proteolytic activation of CREB3L1 in human A549 cells by inhibition of TM4SF20 expression. Normally, TM4SF20 acts as an inhibitory protein for the RIP of CREB3L1, and TGF-β inhibits TM4SF20 expression

through an extracellular signal-regulated kinase (ERK) dependent pathway (Chen et al., 2014).

Membrane Protein Biosynthesis

In mammalian cells, proteins are targeted to the lumen of the ER through their N-terminal signal peptide (Zimmerman et al., 2011). Signal sequences are located at the N-terminus of proteins and these signal sequences usually contain a stretch of hydrophobic amino acids. It is thought that membrane proteins are translationally co-translocated into the ER membrane (Shao and Hegde, 2011). During translational co-translocation, the signal sequence within a nascent polypeptide is recognized by the signal recognition particle (SRP), and targeted to the ER membrane through the SRP receptor. This targeting reaction enables the transferring of the polypeptide chain through the Sec61 translocation channel (Shao and Hegde, 2011). It has been hypothesized that proteins which are associated with the ER translocation channel Sec61 may be involved in regulating the translocation of inefficient signal sequences across the ER membrane (Hegde and Kang, 2008). For membrane proteins with a signal sequence, the N-terminus of the protein is luminal while the N-terminus of membrane proteins without a signal sequence is cytosolic (Hegde and Lingappa, 1997). Currently, it is assumed that the signal sequence is always active, and that membrane proteins always adopt the same topology as determined by the signal sequence upon translational co-translation.

Of the various translocation components, the translocating-chain associating membrane (TRAM) proteins could play a role in stimulating the translocation of proteins with weak signal sequences that are less hydrophobic (Shao and Hegde, 2011; Voigt et

al., 1996). One of these proteins is TRAM1 (Görlich et al., 1992; Görlich and Rapoport, 1993), which is able to facilitate the targeting of proteins to the ER membrane by artificial signal sequences less hydrophobic than the typical signal peptide (Voigt et al., 1996). Mammalian cells express three TRAM proteins: TRAM1, TRAM2 and TRAM1L1. Sequence alignment show that TRAM proteins share a TRAM-Lag1p-CLN8 (TLC) domain with ceramide synthase, and the domain is also thought to bind ceramide or its related sphingolipids (Winter and Ponting, 2002). The TLC/potential ceramide binding domain could be of great interest as this suggests ceramide regulation of protein translocation.

Scope of Current Study

The scope of this study is to characterize the function of TM4SF20 as it relates to the regulation of CREB3L1 RIP and to determine the mechanism by which TM4SF20 is regulated. This will clarify the role of TM4SF20 membrane topology in the regulation of CREB3L1 RIP and will determine the mechanism by which different forms of TM4SF20 are synthesized and their roles in CREB3L1 RIP.

CHAPTER TWO
Results

Introduction

In a previous study, it was reported that TGF-β stimulated the proteolytic activation of of CREB3L1 by inhibiting the expression of TM4SF20 in A549 cells, a line of human lung cancer cells (Chen et al., 2014). As ceramide was previously shown to induced cleavage of CREB3L1 (Denard et al., 2012), we determined the effect of ceramide on TM4SF20 expression and CREB3L1 RIP. Here we show that the treatment of A549 cells with C_6-ceramide, a cell permeable analogue of ceramide, results in the RIP of CREB3L1, but did not affect the expression levels of TM4SF20. Rather, the results indicated that ceramide treatment produced another form of TM4SF20 with a different membrane topology opposite to that of TM4SF20 produced normally.

Results

Ceramide induces a higher molecular weight form of TM4SF20

We previously reported that TGF-β stimulated the cleavage of CREB3L1 through inhibiting the expression of TM4SF20 in A549 cells (Chen et al., 2014). Since ceramide also induced the cleavage of CREB3L1 (Denard et al., 2012), we expected that ceramide would also reduce the expression of TM4SF20 mRNA if the two factors function to trigger CREB3L1 RIP through the same mechanism. In order to determine the effect of

ceramide treatment on TM4SF20 expression, we utilized a cell permeable analogue of ceramide, C_6-ceramide, to treat cells. It has been previously reported that C_6-ceramide was converted to naturally-existing ceramide in cells through the ceramide synthesis pathway (Denard et al., 2012; Kitatani et al., 2008). Treatment of cells with C_6-ceramide resulted in the cleavage of CREB3L1 as indicated by the appearance of a cleaved nuclear form of CREB3L1 in immunoblots with an antibody against the N-terminal domain of the protein (Figure 1A). However, unlike TGF-β , ceramide did not lower the amount of TM4SF20 mRNA (Figure 1B). Unchanged expression of TM4SF20 under ceramide treatment indicates that ceramide and TGF-β induce cleavage of CREB3L1 through different mechanisms.

Further evidence that ceramide stimulates cleavage of CREB3L1 through a mechanism different from that of TGF-β came from analysis of CREB3L1 cleavage in A549/pTM4SF20 cells. In these cells, the expression of a stably transfected TM4SF20 tagged with a five repeat tandem Myc epitope at the C-terminus is driven by a constitutive promoter such that cleavage of CREB3L1 cannot be stimulated by TGF-β (Chen et al., 2014). However, C_6-ceramide still induced CREB3L1 cleavage in the A549/pTM4SF20 cells (Figure 1C, 1st panel, lanes 3 and 4). Instead of a reduction in the amount of TM4SF20, ceramide treatment produced a new form of TM4SF20 with a higher molecular weight. In untreated cells, TM4SF20 migrated on immunoblot as a single band close to its predicted molecular mass (25 kDa) (TM4SF20(A), Figure 1C, 4th panel, lane 1); after ceramide treatment, a new form of TM4SF20 migrating at ~45 kDa appears (TM4SF20(B), Figure 1C, 4th panel, lanes 3 and 4). The appearance of

TM4SF20(B) correlated with the generation of the nuclear form of CREB3L1 (Figure 1C).

In order to confirm that the appearance of TM4SF20(B) was induced by naturally-existing ceramide and was not an artifact of C_6-ceramide treatment, we treated the cells with other reagents that would also stimulate the endogenous production of naturally-existing ceramides. If the formation of TM4SF20(B) was due specifically to ceramide, then treatment by various reagents stimulating TM4SF20(B) will all demonstrate an increased amount of cellular ceramide. The first treatment was with bacterial sphingomyelinase which hydrolyzes plasma membrane sphingomyelin in cells to produce ceramide (Figure 1D). When cells were treated with sphingomyelinase, TM4SF20(B) was generated and cleavage of CREB3L1 was induced. In untreated cells, TM4SF20 indicated as TM4SF20(A)(Figure 1D, 4th panel, lane 1). With sphingomyelinase treatment TM4SF20(B) was detected in treatments with durations as brief as 0.5 h, (Figure 1D, 4th panel, lanes 2, 3, and 4). The appearance of TM4SF20(B) with sphingomyelinase treatment also correlated with the generation of the nuclear form of CREB3L1 (Figure 1D 1st panel, lanes 2, 3, and 4). Doxorubicin is also known to stimulate the cleavage of CREB3L1 by enhancing the *de novo* synthesis of creamide (Denard et al., 2012). Doxorubicin treatment was also able to stimulate the production of TM4SF20(B) (Figure 1E, 1st panel, lane 2).

To confirm that the only lipids significantly changing in our cells under various treatments, we subjected A549 cells to treatments with: C_6-ceramide, doxorubicin, and sphingomyelinase as before. The cells were then subsequently submitted for liquid

chromatography–mass spectrometry measurement of the sphingolipid profiles. In the sphingolipid profile, the only lipids for which all of the reagents caused a specific and greater than 2-fold change in lipid amounts measured were ceramides (data not shown).

TM4SF20 can be N-glycosylated

To determine the post-translational modifications responsible for the molecular weight shift of TM4SF20(B) we conducted an analysis of N-linked glycosylation in TM4SF20. TM4SF20 belongs to a family of proteins containing four transmembrane domains (Wright et al., 2000), and hydropathy analysis clearly showed four hydrophobic peaks that correspond to the transmembrane helices (Figure 2A). There are four consensus N-linked glycosylation sites in TM4SF20: one (N80) in loop 2 between the predicted 2^{nd} and 3^{rd} transmembrane helices, with three more N-linked glycosylation sites (N132, 148, and 163) in loop 3 between the predicted 3^{rd} and 4^{th} transmembrance helices (Figure 2A, N in red text). While N80 is unlikely to be glycosylated because the amino acid residue is too close to the predicted transmembrane helix (Nilsson and von Heijne, 1993), that still leaves three possible N-glycosylation sites as a possible reason for the shift of TM4SF20(A) from ~22kDa to TM4SF20(B) ~45kDa on immunoblots.

To monitor the glycosylation status of the consensus N-linked glycosylation sites of TM4SF20, we incubated the whole cell lysates of C_6-ceramide -treated A549/pTM4SF20-Myc cells with Endoglycosidase H (endo H) and Peptide-N-Glycosidase F (PNGase F). Endo H and PNGase F are two different endoglycosyidases, where Endo H only removes high mannose and some hybrid N-linked carbohydrates, PNGase F removes almost all types of N-linked glycosylation. Deglycosylation treatment

with both enzymes reduced the apparent molecular weight of TM4SF20(B) but not that of TM4SF20(A) (Figure 2B, 1st panel, lanes 2 and 3). The reduction in molecular weight of TM4SF20(B) while TM4SF20(A) remained unchanged indicated that only TM4SF20(B) is glycosylated. Simultaneous replacement of all three asparagines in possible glycosylation sites of TM4SF20, N80, N132, 148, and 163 by site-directed mutagenesis to glutamines reduced the apparent molecular weight of TM4SF20(B) to that of the wild type protein treated with PNGase F (Figure 2C, 1st panel, lanes 13 and 14). The apparent molecular weight reduction of the triple mutant N132Q, N148Q, and N163 TM4SF20(B) suggests that those three sites are the only N-linked glycosylation sites in TM4SF20(B). In contrast to these sites located in loop 3, N80 located in loop 2, is not glycosylated in TM4SF20(B) as the N80Q mutation did not alter the migration of the protein (Figure 2C, lanes 3 and 5). This site is not glycosylated in TM4SF20(A), presumably because it is too close to the predicted transmembrane helix (Nilsson and von Heijne, 1993). We noticed that the deglycosylation treatment did not completely reduce the apparent molecular weight to that of TM4SF20(A), suggesting that TM4SF20(B) may contain additional post translational modifications.

Ceramide appears to specifically alter the glycosylation of pattern of TM4SF20, as C_6-ceramide treatment did not change the glycosylation pattern of either Grp97, an ER luminal protein, or that of NPC1, a transmembrane protein (data not shown).

Ceramide-induced TM4SF2(B) has an entirely opposite membrane topology

Since N-linked glycosylation can only occur in the lumen of the ER (Breitling and Aebit, 2013), the results shown thus far all suggests that the loop between the predicted

3rd and 4th transmembrane helices of TM4SF20(B) containing all three glycosylation sites must be located in the ER lumen. Conversely, the same loop in TM4SF20(A) would have to be exposed to the cytosol instead, as that protein is not glycosylated. If this is the case, then the C-terminal end of the protein which is separated from the loop by a single transmembrane helix should be in the ER lumen for TM4SF20(A), but in the cytosol for TM4SF20(B).

In order to test this the location of the C-terminus of both TM4SF20(A) and TM4SF20(B) we performed a protease protection assay. If the C-terminal of TM4SF20(A) is in the ER lumen, then the Myc epitope tagged at the C-terminus should be protected from protease K digestion by microsomes, and only be digested when microsomes are disrupted with the addition of a detergent; while TM4SF20(B) should demonstrate no protection from digestion as its C-terminus is predicted to be in the cytosol and always exposed to protease K digestion. As shown in Figure 2D, the Myc epitope at the C-terminus of TM4SF20(A) but not TM4SF20(B) was protected from protease digestion by microsomes. TM4SF20(A) was detectable at protease K treatments up to 3 µg/ml added to the microsomes (Figure 2D, lanes 1-6), and is only exposed to enzymatic digestion in the presence of NP-40 (Figure 2D, lanes 7 and 8). The C-terminal Myc epitope of TM4SF20(B) was always exposed to digestion in the protease protection assay, as even without disruption of the microsomes by a detergent, the TM4SF20(B) form was not protected from protease K (Figure 2D, lanes 1 and 2). The protease K protection assay was also performed on a N-terminal Myc epitope tagged form of TM4SF20(B). If the N-terminal of TM4SF20(B) is not protected , then the Myc epitope

detected in immunoblots will decrease upon treatment with protease K. Similar to the C-terminal Myc-tagged TM4SF20(B), the N-terminal Myc epitope tagged form of TM4SF20(B) did not demonstrate significant protection from protease K digestion by microsomes (Figure 2E, lanes 1 and 2, 7 and 8), suggesting that the N-terminus of TM4SF20(B) is also in the cytosol.

The results of the protease K protection assay suggests that the membrane topology of TM4SF20(B) seen in response to ceramide accumulation is opposite from that of TM4SF20(A) existing under normal conditions.

Ceramide prevents the N-terminal sequence of TM4SF20 from cleavage by signal peptidase

In contrast to the C-terminally tagged Myc epitope which allows the detection of both forms of TM4SF20, the N-terminally tagged Myc epitope can only detect TM4SF20(B). A possible explanation for the inability to detect a N-terminally Myc epitope tagged form of TM4SF20(A) was that the N-terminal sequence of TM4SF20(A) but not TM4SF20(B) is forced to function like a signal peptide such that the N-terminal sequence and the N-terminal Myc epitope tag was co-translationally removed from the mature protein by signal peptidase. To test whether signal peptidase was responsible for removing the N-terminal sequence of TM4SF20(A) along with the N-terminal Myc epitope, we transfected cells with a siRNA duplex targeting the signal peptidase complex subunit 3 (SPCS3), a component of signal peptidase (Meyer and Harmann, 1997). After the siRNA transfection, we then also transfected a plasmid encoding TM4SF20 tagged with the Myc epitope at the N-terminus. The siRNA knockdown of SPCS3 was more

than 90% (Figure 3B), and resulted in the generation a form of TM4SF20 detectable by the N-terminally tagged Myc epitope of TM4SF20(A) (Figure 3C, 2nd panel, lanes 3 and 4). This N-terminal Myc tagged form of TM4SF20(A) detected had a higher apparent molecular weight than that of C-terminally Myc epitope tagged TM4SF20(A) observed in cells transfected with a plasmid encoding C-terminally tagged TM4SF20 (Figure 3C, 2nd panel, lanes 3, 4, and 5). The N-terminal Myc epitope tagged form of TM4SF20(A) detectable after siRNA knockdown of SPCS3 expression has been designated "pre-TM4SF20(A)."

To confirm retention of the N-terminal Myc tag in pre-TM4SF20(A) was due to the SPCS3 knockdown, we performed a SPCS3 complementation experiment. First, we transfected cells with siRNA targeting SPCS3 as before, and then transfected cells with the N-terminal Myc epitope tagged TM4SF20 or co-transfected it with a plasmid containing cDNA encoding a SPCS3 with synonymous mutations at the region targeted by the siRNA. The knockdown of SPCS3 again resulted in the formation of a pre-TM4SF20(A) with a larger apparent molecular weight than TM4SF20(A) (Figure 3C, 1st panel, lanes 1 and 2). The co-transfection of SPCS3 with the N-terminally tagged TM4SF20 was able to restore expression of SPCS3 (Figure 3D). With the restoration of SPCS3 by co-transfection the pre-TMSF20(A) band disappeared (Figure 3C, 1st panel, lanes 2, 4, and 5). This result suggests that the N-terminal sequence of TM4SF20 can indeed be processed and cleaved by signal peptidase. The co-translational processing of the N-terminus of TM4SF20 would explain the inability to detect N-terminally Myc

epitope tagged form of TM4SF20(A) in immunoblot as the N-terminal sequence of TM4SF20 is processed by signal peptidase and removed from TM4SF20(A).

Calculation of the difference in molecular weight between pre-TM4SF20(A) and TM4SF20(A) suggested that the N-terminal 13-15 amino acids constitute a region in pre-TM4SF20(A) which may behave like a signal peptide that is normally removed from the mature protein. To identify the specific cleavage site more precisely, we took advantage of previous observations that proline is intolerable to signal peptidase at the P1' site, and the presence of a proline at the C-terminus of cleaved peptide bond results in the inability of signal peptidase to cleave at that site (Choo and Ranganathan, 2008; Nilsson and Von Heijne, 1992). Mutations of each individual amino acids from residues 12 to 16 to proline in a C-terminally Myc epitope tagged TM4SF20 plasmid were made to determine which mutation would block the signal peptidase cleavage of the pre-TM4SF20(A) form, and permit accumulation of the pre-TM4SF20(A) form. None of the mutations made affected the ability of ceramide to induce TM4SF20(B) production (Figure 3E, 1st panel). Pre-TM4SF20(A) was only detectable in the immunoblot of TM4SF20(S14P) in the immunoblot against the Myc epitope tagged at the N-terminus of the protein (Figure 3F, 2nd panel, lane 7). This result indicates that the signal peptidase cleaved TM4SF20(A) between F13 and S14.

Ceramide-induced TM4SF20(B) is newly synthesized in response to ceramide

As membrane proteins are inserted into membranes during translation, we speculated that the TM4SF20(B) form is likely to be newly synthesized upon stimulation with ceramide instead of being previously extant TM4SF20(A) that adopted a different

membrane topology orientation in the presence of ceramide. In order to test this, we treated cells with C_6-ceramide with or without cycloheximide, an inhibitor for protein synthesis. The inhibition of protein synthesis by cycloheximide prevented the formation of TM4SF20(B) in the presence of ceramide (Figure 4A, 1st panel, lanes 2 and 4). However, cycloheximide did not reduce the amount of TM4SF20(A) seen in cells treated with C_6-ceramide (Figure 4A, 1st panel, lanes 3 and 4), suggesting that the TM4SF20(A) observed in ceramide-treated cells was likely synthesized before the addition of C_6-ceramide (Figure 1C, 1D, 1E), and that TM4SF20(B) is protein newly synthesized by cells in response to lipid treatment.

In order to confirm that TM4SF20(B) is newly synthesized protein from ceramide treatment, we performed ^{35}S-methionine labeling of TM4SF20, and chased in the presence or absence of C_6-ceramide. If TM4SF20(B) is newly synthesized in response to ceramide treatment, then it would be expected that ^{35}S-methionine will only label TM4SF20(A) form. In cells transfected with a C-terminally Myc epitope tagged TM4SF20, we were able to detect a band corresponding to the molecular weight of TM4SF20(A) in the phosphor image (Figure 4B, 1st panel, lanes 2 and 3) as well as in the immunoblot against the Myc epitope (Figure 4B, 2nd panel , lanes 2 and 3). The ceramide-induced production of TM4SF20(B) was detectable in the immunoblot (Figure 4B, 2nd panel, lane 3), but there was no corresponding increased ^{35}S signal in the phosphor image at the molecular weight corresponding to TM4SF20(B). This result also indicates that TM4SF20(B) is newly synthesized in the presence of ceramide, and that the

membrane topology of TM4SF20(A) is not altered in response to treatment with ceramide.

To rule out the possibility that the results shown in Figure 4A was due to the ceramide-mediated stabilization of TM4SF20(B), cells were treated with or without the cell-permeable proteasome inhibitor, MG-132, and then treated with C_6-ceramide. If TM4SF20(B) detected in the presence of ceramide was due to stabilization, then MG-132 treatment of A549/pTM4SF20 would result in detectable TM4SF20(B) without ceramide treatment. In the absence of MG-132, TM4SF20(B) is only detected when A549/pTM4SF20 cells are treated with C_6-ceramide (Figure 4C, 1st panel, lanes 1 and 2). MG-132 treatment did not result in a stabilization of TM4SF20(B) (Figure 4C, 1st panel, lanes 3 and 4). The lack of accumulation of TM4SF20(B) when cells are treated with MG-132 but not with C_6-ceramide further supports previous data indicating that TM4SF20(B) is newly synthesized in response to lipid treatment, and that the increase of TM4SF20(B) detected after ceramide treatments is not due to a ceramide-mediated stabilization event.

Ceramide alters membrane topology of TM4SF20

The results presented thus far is summarized as a model in Figure 5 and shows the two forms of TM4SF20 revealed. In the absence of ceramide the N-terminal signal sequence of TM4SF20 translocates through the membrane and is cleaved in the lumen by signal peptidase. In this form of TM4SF20, designated as TM4SF20(A), the N-terminus of the mature protein lies in the lumen. The B form of TM4SF20 is induced by ceramide, and the N-terminal sequence is not treated as a signal peptide; it does not cross the

membrane and is not cleaved. The protein designated as TM4SF20(B) adopts a topology opposite to that of TM4SF20(A). Exposed loops that are cytosolic in TM4SF20(A) are luminal in TM4SF20(B) and vice versa.

Alternative translocation of TM4SF20 depends on the 1st transmembrane helix of the protein

In order to determine if the N-terminus of TM4SF20 could function as a signal sequence, we replaced the signal sequence of Myc epitope tagged human placental alkaline phosphatase (AP) with the first 13 amino acids of TM4SF20. We then transfected both the TM4SF20(1-13)-AP(23-507)-Myc plasmid construct and a construct containing AP(1-507)-Myc, a plasmid containing cDNA encoding alkaline phosphatase with its own signal sequence intact into A549 cells. Transfected cells were then harvested, the lysates subjected to PNGase F treatment, and immunoblot analysis. Alkaline phosphatase has two N-linked glycosylation sites at amino acids 144 and 271. Alkaline phosphatase with its own signal sequence intact should be inserted into the membrane such that the glycosylation sites of AP are in the ER lumen and available for glycosylation. If the first 13 amino acids at the N-terminus of TM4SF20 can function as a signal sequence, then the TM4SF20(1-13)-AP(23-507)-Myc fusion protein would be synthesized such that the AP portion is in the lumen and glycosolated. When AP(1-507)-Myc is treated with the endoglycosidase PNGase F, the apparent molecular weight of PNGase F treated AP(1-507) decreased (Figure 6A, lanes 3 and 4), indicating that the signal sequence of AP(1-507)-Myc functioned to place the transfected AP with the glycosylation sites exposed to the ER lumen. However, no shift in apparent molecular

weight from the deglycosylation treatment was seen for the fusion protein TM4SF20(1-13)-AP(23-507)-Myc (Figure 6A, lanes 5 and 6), suggesting that the N-terminus of TM4SF20 is not a signal sequence.

We then replaced the first 14 amino acid residues at the N-terminus of TM4SF20 with the signal sequence of prolactin in order to determine if the signal sequence of prolactin was sufficient to alter the ability of TM4SF20 to alternatively translocate. Alternative translocation continued to be stimulated by ceramide, with the generation of a TM4SF20(B) form seen when cells were treated with C_6 ceramide (Figure 6B, 1st panel, lanes 3 and 4). This result indicated that alternative translocation of TM4SF20 is likely to be determined by the other domains of TM4SF20.

Since the immediate N-terminal sequence of TM4SF20 does not appear to function as a signal sequence, we then focused on the first transmembrane helix immediately following that region. This transmembrane helix contains two residues, glycine 22(G22) and asparagine 26(N26) that do not belong in the stretch of much more hydrophobic amino acid residues in the transmembrane helix (Figure 5, in red text). To determine the role of the polar residues in TM4SF20, we mutated each residue to leucine. As before, only TM4SF20(B) was detected by immunoblot for N-terminally Myc-tagged wild type TM4SF20 in cells treated with ceramide (Figure 6C, lanes 3 and 4). In contrast, the N-terminally Myc-tagged TM4SF20(N26L)(B) was readily visible even without ceramide treatment (Figure 6C, 1st panel, lanes 5 and 6). The C-terminally Myc-tagged TM4SF20(N26L) mutant was detected as the B form without ceramide treatment, and the A form was completely undetectable (Figure 6C, 1st panel, lanes 9 and 10), unlike the

wild type TM4SF20-Myc which exists as the A form in conditions without ceramide, and both A and B can be seen upon ceramide treatment (Figure 6C, 1st panel, lanes 7 and 8). The same results were observed for TM4SF20(G22L), where the TM4SF20(G22L) mutant was detected as the B form without ceramide, and the A form was completely undetectable (Figure 6D). Together, these results suggest that glycine 22 and asparagine 26 within the first transmembrane helix of TM4SF20 are required for the ability of TM4SF20 to respond to ceramide-induced alternative translocation, and that it is the first transmembrane helix which determines the orientation of TM4SF20 as it passes through ER translocon.

In order to investigate the properties of the first transmembrane helix of TM4SF20 responsible for determining its membrane topology, the amino acid residue G22 was mutated by site-directed mutagenesis to a number of different amino acids and assayed by immunoblot as demonstrated before in figures 6C and 6D. The mutation of glycine 22 to: tryptophan (7A, 1st panel, lanes 7 and 8), phenylalanine (7B, 1st panel, lanes 9 and 10), tyrosine (7B, 1st panel, lanes 13 and 14), valine (7C, 1st panel lanes 5 and 6), asparagine (7C, 1st panel, lanes 7 and 8), isoleucine (7C, 1st panel, lanes 9 and 10); all eliminated the ceramide-regulated alternative translocation of TM4SF20 such that only the TM4SF20(B) form could be detected. Of the mutations tested for G22, only mutations of glycine 22 to alanine or serine left the protein TM4SF20 still able to alternative translocate in a ceramide-regulated manner. These results suggest that bulky residues are not tolerated in this position for ceramide to induce alternative translocation of TM4SF20.

The amino acid residue asparagine 26 was also mutated by site-directed mutagenesis to a number of different amino acids and assayed by immunoblot to determine the mutations which can be tolerated by TM4SF20 such that TM4Sf20 still retained ceramide-induced alternative translocation. For asparagine 26, mutations to: glycine (7D, 1st panel, lanes 7 and 8), alanine (E, 1st panel, lanes 7 and 8), glutamine (7E, 1st panel, lanes 9 and 10), and serine (7E, 1st panel, lanes 11 and 12) all resulted in a disruption of alternative translocation in response to ceramide such that only the TM4SF20(B) form can be detected when N26 is mutated. These results indicated that asparagine at position 26 in the first transmembrane helix of TM4SF20 is required for ceramide-regulated alternative translocation.

The N-terminus of TM4SF20 encompassing the first transmembrane domain is sufficient to induce alternative translocation.

To determine if the first transmembrane helix of TM4SF20 is sufficient to induce alternative translocation, the signal sequence from alkaline phosphate was replaced with the N-terminal 36 amino acids of TM4SF20 containing the first transmembrane domain, and tagged the fusion protein with the Myc epitope at the C-terminus. The AP protein is usually a secreted an glycosylated protein (Sakai et al., 1998), but with the AP signal sequence deleted and replaced with the N-terminal sequence derived from TM4SF20, the membrane orientation should be determined by that N-terminal TM4SF20 sequence.

The model shown in Figure 8A predicts the localization of the TM4SF20-AP-Myc fusion protein based on the hypothesis that the N-terminal sequence of TM4SF20 including the first transmembrane domain is necessary to induce alternative translocation

in response to ceramide: the AP portion of the protein is expected to reside in the cytosol in the absence of ceramide so that the protein should not be glycosylated, and the C-terminal Myc tag would not be protected by microsomes (Figure 8A, left panel, "Fusion Protein A"). Should ceramide treatment induce alternative translocation of the fusion TM4SF20-AP protein, then the AP portion is expected to be in the ER lumen, glycosylated, and the C-terminal Myc tag would be protected from protease digestion from microsomes (Figure 8A, right panel, "Fusion Protein B").

In order to test if TM4SF20-AP-Myc fusion protein behaved as predicted in the model (Figure 8A), cells were transfected, treated with or without ceramide, the cell lysates incubated with PNGase F, and subjected to immunoblot analysis. In the absence of ceramide, the fusion protein migrated as two bands in an immunoblot against the C-terminal Myc tag of the fusion protein (Figure 8B, lane 1). The higher of the two fusion protein bands seen was glycosylated, as treatment with PNGase F reduced its apparent molecular weight in immunoblots (Figure 8B, lanes 1 and 2). The C-terminal Myc tag on the glycosylated form of the fusion protein was protected from protease digestion by intact microsomes (Figure 8C), indicating that this band represented the B form of the fusion protein as illustrated in the model in Figure 8A. The lower band seen of the fusion protein was not glycosylated, as PNGase F treatment did not further reduce the apparent molecular weight (Figure 8B, lanes 1 and 2). Additionally, it was also unprotected from protease digestion by microsomes (Figure 8C), indicating that this band was the A form of the fusion protein.

In testing the behavior of the TM4SF20-AP-Myc fusion protein, we observed that

C_6-ceramide treatment increased the amount of B form of the fusion protein but not that of the A form in immunoblots (Figure 8B, lanes 3 and 4), which suggested that ceramide treatment also induced alternative translocation of the fusion protein as predicted by the model shown in Figure 8A. However, unlike TM4SF20 which only existed as the A form in the absence of ceramide, the TM4SF20-AP-Myc fusion protein existed as both the A and B forms in this condition (Figure 8B, lane 1). The results of the TM4SF20-AP-Myc fusion protein experiments suggest that the inclusion of the first transmembrane domain to a fusion protein is necessary for the N-terminus of TM4SF20 to function in ceramide-induced alternative translocation. As the N-terminus of TM4SF20 does not function as a signal sequence, and it is the first transmembrane domain that is needed for alternative translocation, components of the ER translocon may play a greater role in this mechanism.

Ceramide induces alternative translocation of TM4SF20 by dissociating TRAM2 from the ER translocon

In order to test if TRAM1 is required for the ability of the ER translocon to use the N-terminal sequence of TM4SF20 as a signal peptide, and if ceramide triggers alternative translocation of the protein through the inactivation of TRAM1, siRNA knockdown of TRAM1 was performed. However, knockdown of TRAM1 by more than 90% with two different siRNA did not affect the ceramide-induced alternative translocation of TM4SF20 (data not shown). Mammalian cells express two homologues of TRAM1, namely TRAM1L1 and TRAM2. Since A549 cells only express TRAM1 and TRAM2, but not TRAM1L1, we determined if this protein was required for the

alternative translocation of TM4SF20 by performing a knockdown. Knocking down TRAM2 by ~70% with two different siRNA (Figure 9A) produced TM4SF20(B) even without the addition of excess ceramide in the form of C_6-ceramide treatment (Figure 9B). This result suggests that TRAM2 is required for the N-terminal sequence of pre-TM4SF20(A) to be treated as a signal peptide by the ER translocon such that the protein is synthesized and inserted into the membrane properly under normal conditions, as knockdown of TRAM2 promoted the generation of TM4SF20(B) even in the absence of ceramide.

To confirm that it was the knockdown of TRAM2 that de-regulated the alternative translocation of TM4SF20 in A549/pTM4SF20 cells, and not an off-target, increase in ceramide levels caused by the TRAM2 knockdown itself, we transfected cells with TRAM2 siRNA, and then arranged for mass spectrometry to be performed on the final cell samples for determination of sphingolipid and ceramide profiles. The results of the mass spectrometry analysis suggests that it is the knockdown of TRAM2 that causes the alternative translocation of TM4SF20 because ceramide levels of all detectable ceramide chain lengths were not significantly different between the control and TRAM2 knockdown samples (data not shown).

A simple hypothesis based on the TRAM2 knockdown data and the resultant formation of TM4SF20(B) would be that accumulation of ceramide in the ER may dissociate TRAM2 from Sec61 by binding to TRAM2 through the TLC domain. In order to test this hypothesis, we transfected cells with plasmids encoding epitope-tagged TRAM2 and Sec61, immunoprecipitated the transfected TRAM2 by the Myc epitope tag,

and determined the amount of Sec61 that was co-immunoprecipitated. In the absence of ceramide, Sec61 co-immunoprecipitated with TRAM2 (Figure 9C, lane 3). Compared to the amount of Sec61 co-immunoprecipitated with TRAM2, the amount of Sec61 was markedly decreased in cells that were treated with C_6-ceramide (Figure 9C, lane 4). This result suggests that ceramide inactivates TRAM2 by dissociating the protein from the ER translocon complex. The dissociation of TRAM2 from the ER translocon then results in the de-regulated translocation of TM4SF20 during translation to produce TM4SF20(B) even in the absence of ceramide.

TM4SF20(B) stimulates CREB3L1 cleavage

The results in Figure 1 demonstrate that the appearance of TM4SF20(B) correlates with the generation of the nuclear form of CREB3L1 through RIP. If TM4SF20(B) is a trigger of CREB3L1 cleavage, then treatments producing TM4SF20(B) other than those causing the accumulation of ceramide should trigger CREB3L1 cleavage as well.

In order to test whether the presence of TM4SF20(B) could trigger CREB3L1 cleavage, we took advantage of the TM4SF20 mutant shown in Figure 6 to always alternatively translocate and express solely as TM4SF20(B) regardless of ceramide treatment. To determine whether over-expression of TM4SF20(G22L) could cause cleavage of CREB3L1 even in the absence of ceramide, lentivirus encoding either wild type or the G22L mutant of TM4SF20 was generated and used to infect A549 cells. Virus encoding green fluorescent protein (GFP) was used as a control for effects of the virus infection and transduction process. Neither infection with the control GFP virus nor the

wild type TM4SF20 virus affected the ceramide-induced cleavage of CREB3L1Cells infected with either GFP or wild type TM4SF20 virus still displayed ceramide-regulated cleavage of CREB3L1 only when treated with ceramide (Figure 10A, lanes 1-4). In contrast, infection of cells with the virus encoding TM4SF20(G22L) resulted in the cleavage of CREB3L1 even in the absence of ceramide (Figure 10A, lane 5). This result suggests that TM4SF20(B) functions in the cell to stimulate the cleavage of CREB3L1.

A second experiment by which to test if TM4SF20(B) functions to stimulate CREB3L1 RIP was to knockdown TRAM2. TRAM2 knockdowns also caused the alternative translocation of TM4SF20 to produce TM4SF20(B) regardless of ceramide treatment (Figure 9A and 9B). In order to test this, siRNA knockdown of TRAM2 was performed on A549/pTM4SF20 cells, treated with or without ceramide, fractionated, and immunoblot analysis was performed on the nuclear and membrane fractions. In the absence of ceramide treatment, TM4SF20(B) and the nuclear form of CREB3L1 were barely detectable in cells transfected with a control siRNA (Figure 10B, panels 1 and 4, lane 1). However, both TM4SF20(B) and nuclear CREB3L1 become readily detectable in cells transfected with siRNA targeting TRAM2 (Figure 10B, panels 1 and 4, lane 3).

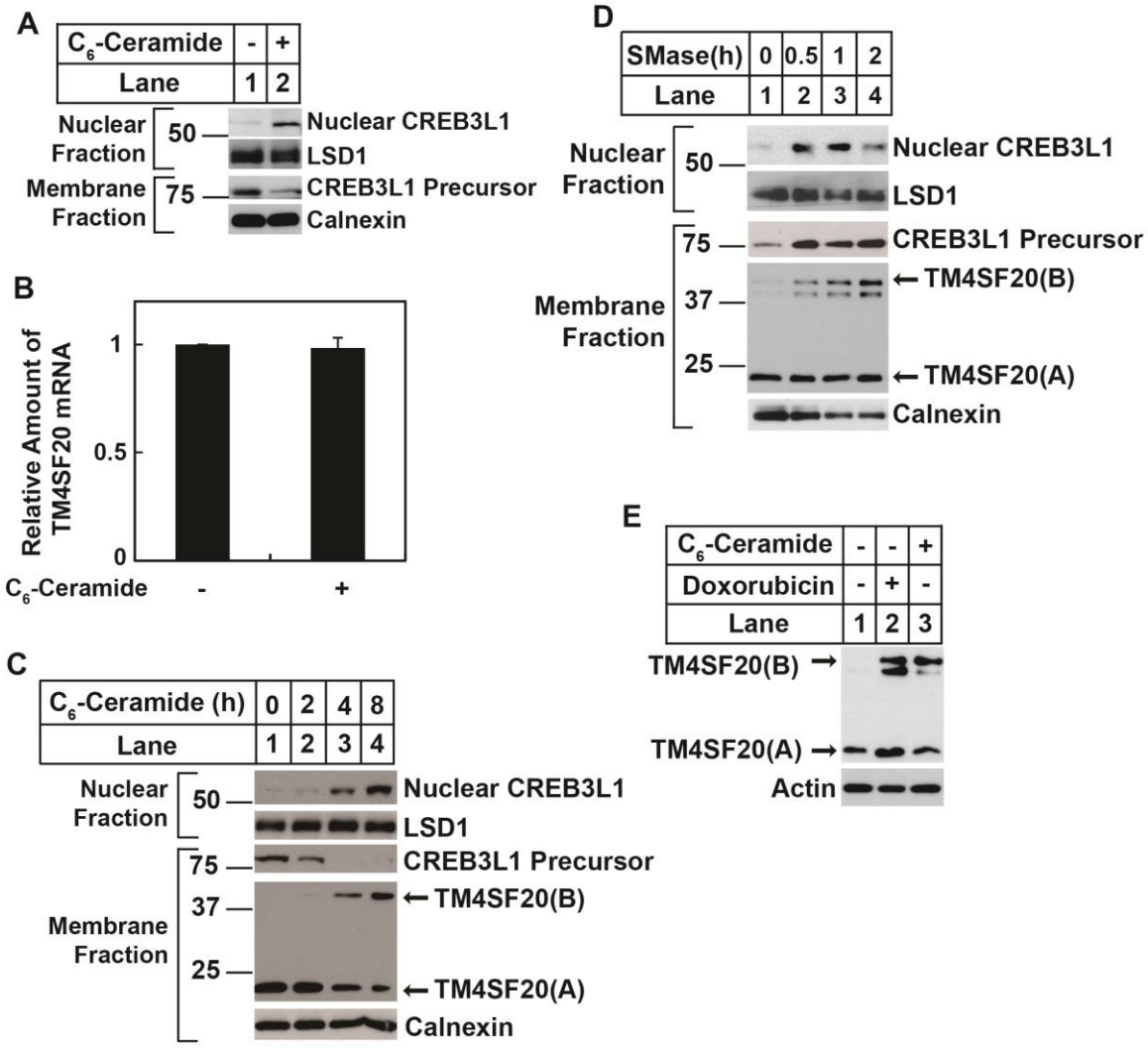

Figure 1. Ceramide Induces the Appearance of a Higher Molecular Weight Form of TM4SF20

(A and B) On day 0, A549 cells were seeded at 4×10^5 cells per 60-mm dish. On day 1, cells were treated with or without 6μM C_6-ceramide for 8 h. (A) Cells were harvested and separated into nuclear and membrane fractions, and analyzed by immunoblot analysis with antibodies as indicated. Immunoblotting with antibodies against calnexin and lysine-specific demethylase 1 (LSD1) served as loading controls for membrane and nuclear fractions. (B) The amount of TM4SF20 mRNA was quantified through RT-QPCR with the value in non-treated cells set to 1. Results are reported as mean ± S.E.M. of three independent experiments.

(C) On day 0, A549/pTM4SF20 cells were seeded at 4×10^5 cells per 60-mm dish. On day 1, cells were treated with 6 μM of C_6-ceramide for the indicated time. Cells were then harvested for analysis of CREB3L1 RIP as described in A. Immunoblot with anti-Myc

was used to detect the stably transfected TM4SF20 tagged with the Myc epitope at the C-terminus of the protein.
(D) On day 0, A549/pTM4SF20 cells were seeded at 4×10^5 cells per 60-mm dish. On day 1, cells were treated with 0.24 units/ml of sphingomyelinase for the indicated time. Cells were then harvested for immunoblot analysis as described in C.
(E) On day 0, A549/pTM4SF20 cells were seeded at 4×10^5 cells per 60-mm dish. On day 1, cells were treated with 500 nM doxorubicin for 24 h, or 6 μM C_6-ceramide for 8 h, followed by harvesting cells for whole cell lysate and immunoblot analysis with the indicated antibodies.

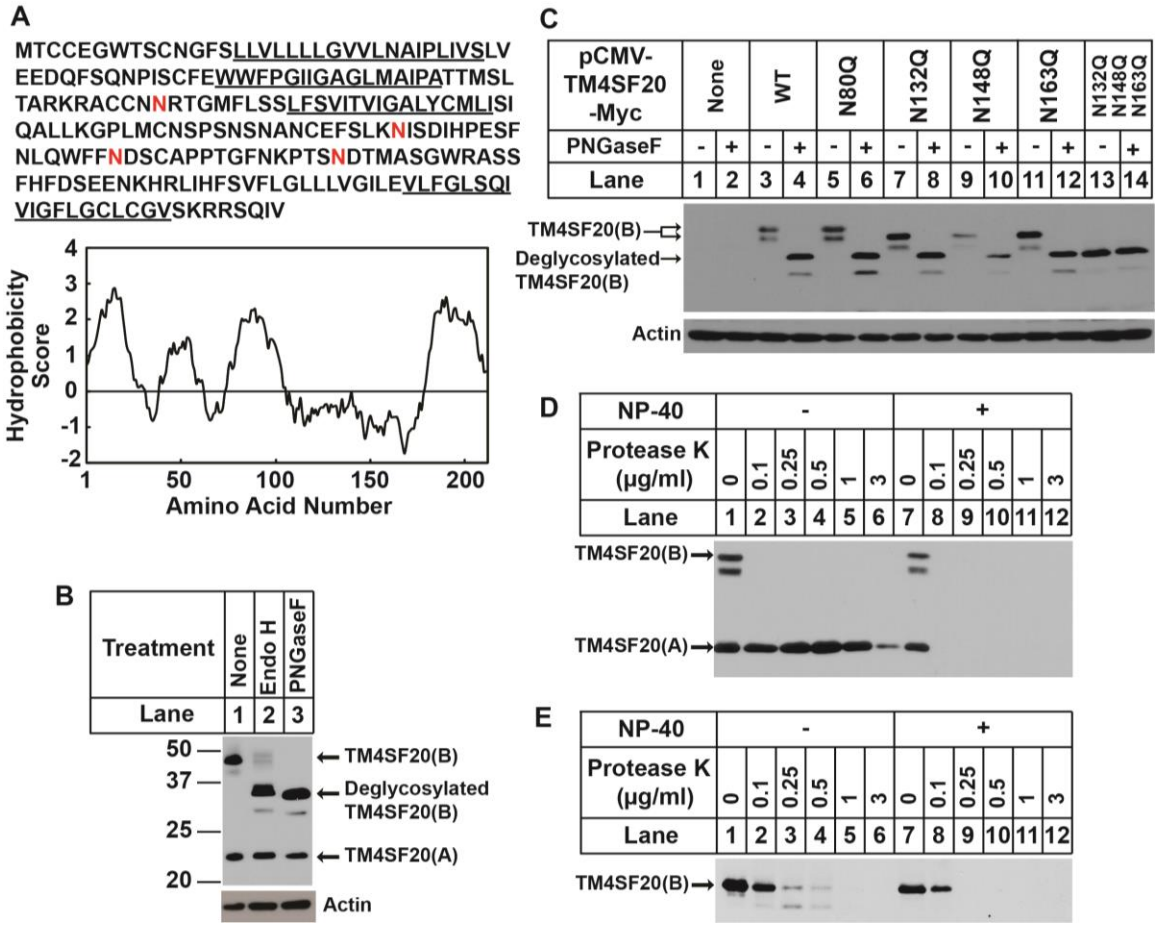

Figure 2. TM4SF20 can be N-glycosylated and Ceramide Alters the Membrane Topology of TM4SF20 (experiments performed by Qiuyue Chen)

(A) The amino acid sequence and hydropathy plot of TM4SF20. The putative membrane-spanning sequences are underlined. Potential N-linked glycosylation sites are highlighted in red. The residue-specific hydropathy index was calculated over a window of 18 residues by the method of Kyte and Doolitte.

(B) On day 0, A549/pTM4SF20 cells were seeded at 4×10^5 cells per 60-mm dish. On day 1, cells were treated with 6 μM C_6-ceramide for 8 h. Cells were then harvested and cell lysates incubated in the absence or presence of indicated glycosidases. Treated lysates were then subject to SDS-PAGE and analyzed by immunoblot with anti-Myc antibody to detect the stably transfected C-terminally Myc-tagged TM4SF20.

(C) On day 0, A549/pTM4SF20 cells were seeded at 4×10^5 cells per 60-mm dish. On day 1, cells were transfected with 0.1 μg of wild type or mutant pCMV-TM4SF20-Myc as indicated, with the total amount of DNA adjusted to 2 μg/dish with empty pcDNA3.1 vector. On day 2, cells were were treated with 6 μM C_6-ceramide for 8 h. Cells were then harvested and lysates incubated in the absence or presence of PNGase F, followed my immunoblot analysis.

(D)) On day 0, A549/pTM4SF20 cells were seeded and treated as described in C. Membrane vesicles were prepared and subjected to protease protection assay as described in Methods followed by immunoblot analysis with anti-Myc detecting the epitope tagged at the C-terminus of TM4SF20.
(E) On day 0, A549/pTM4SF20 cells were seeded at 4×10^5 cells per 60-mm dish. On day 1, cells were transfected with 0.1 ug of pCMV-Myc-TM4SF20 with the total amount of DNA adjusted to 2 µg/dish with empty pcDNA3.1 vector. On day 2, cells were were treated with 6 µM C_6-ceramide for 8 h. Protease protection assay was performed as described in D.

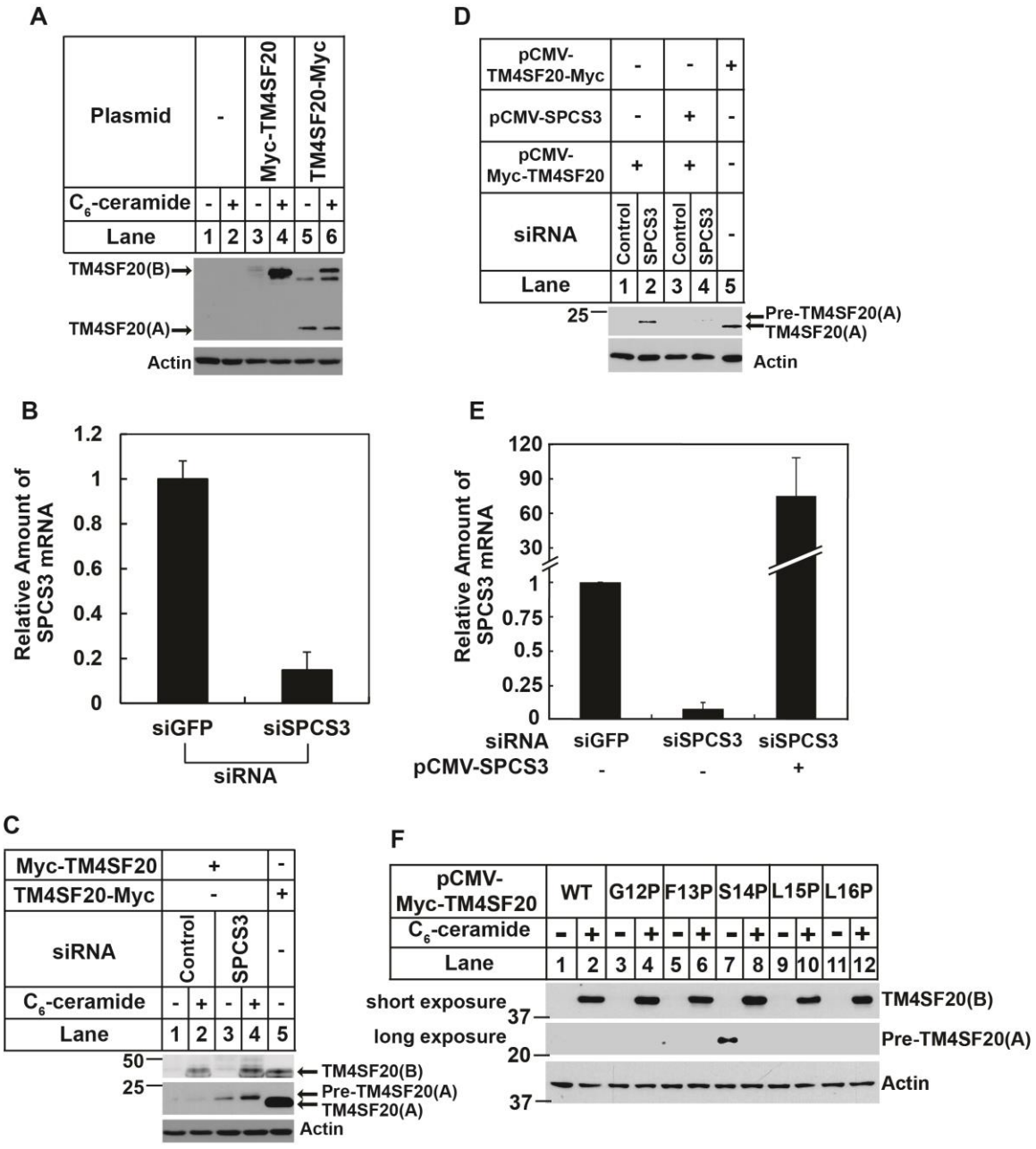

Figure 3. Ceramide Prevents the N-terminal Sequence Cleavage of TM4SF20 by Signal Peptidase

(A) On day 0, A549 cells were seeded at 4×10^5 cells per 60-mm dish. On day 1, cells were transfected with 0.1 μg of pCMV-TM4SF20-Myc or pCMV-Myc-TM4SF20. The total amount of DNA was adjusted to 2 μg/dish with empty pcDNA3.1 vector. On day 2, subjected to immunoblot analysis with anti-Myc for the detection of TM4SF20.

(B, C, D, and E) On day 0, A549 cells were seeded at 1×10^5 cells per 60-mm dish. On

day 1, the cells were transfected with the indicated siRNAs. On day 3, the cells were transfected with 0.1µg of of the indicated plasmids as described in A. On day 4, cells were treated with or without 6 µM of C_6-ceramide for 8 h. (B and E) Then cells were harvested for RNA and quantification of SPCS3 knockdown by RT-QPCR as described in Methods. (C and D) The remaining cells were harvested and subject to analysis as described in A.

(F) On day 0, A549 cells were seeded at 4×10^5 cells per 60-mm dish. On day 1, cells were transfected with 0.1 µg of indicated plasmids as described in A. After incubation for 8 h, cells were then treated with 6 µM of C_6-ceramide for 16 h. On day 2, after 16 h of the C_6-ceramide treatment, cell lysates were subjected to immunoblot analysis with anti-Myc to detect TM4SF20 (experiment performed by Bray Denard).

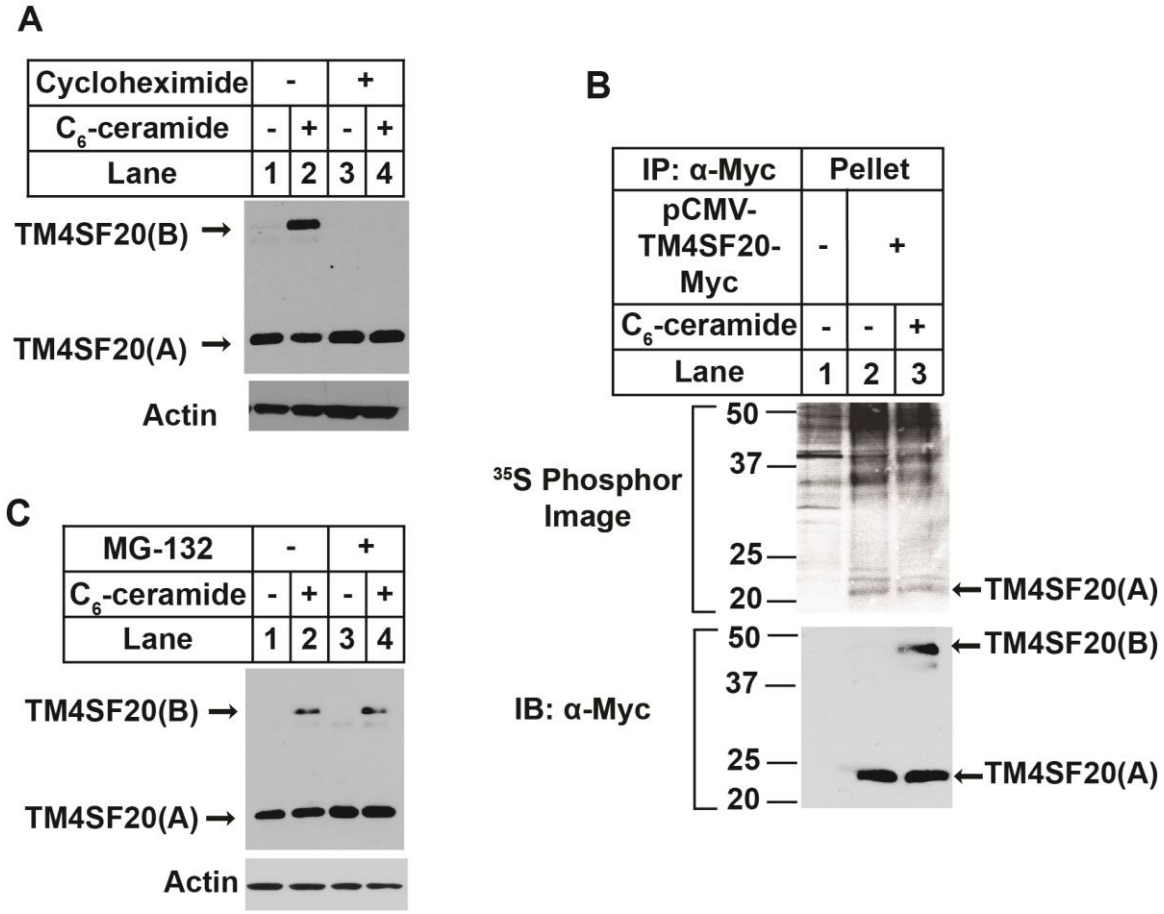

Figure 4. Ceramide-Induced TM4SF20(B) is Newly Synthesized in Response to Ceramide

(A) On day 0, A549/pTM4SF20 cells were seeded at 4×10^5 cells per 60-mm dish. On day 1, cells were treated with 50 µM cycloheximide or 4 µM C_6-ceramide for 5 h. Cell lysates were subjected to immunoblot analysis with anti-Myc in order to detect the C-terminal Myc epitope tagged TM4SF20.

(B) On day 0, SV589 cells were seeded at 4×10^5 cells per 60-mm dish. On day 1, cells were transfected with 0.1 µg of pCMV-TM4SF20-Myc (efficient codon mutant) The total amount of DNA was adjusted to 2 µg/dish with empty pcDNA3.1 vector. On day 2, cells were radiolabelled with 35S-methionine as described in Methods and chased with or without 6 µM C_6-ceramide. Immunoprecipitation of ^{35}S-methionine radiolabelled cell lysates was performed as described in Methods. Final immunoprecipitation samples were subjected to SDS-PAGE and immunoblotting or phosphor screen imaging as appropriate.

(C) On day 0, A549/pTM4SF20 cells were seeded at 4×10^5 cells per 60-mm dish On day 1, cells were treated with or without 4 µM C_6-ceramide for 8 h, and with or without 5 µM MG-132 treatment for 2 h. Cells were then harvested, and lysates subjected to immunoblot analysis.

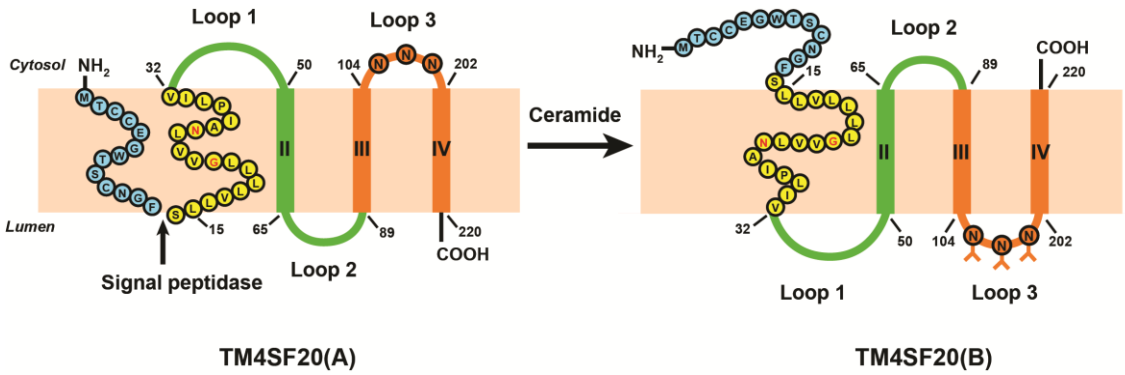

Figure 5. Model Illustrating the Ceramide-Induced Alternative Translocation of TM4SF20

Proposed model illustrating the ceramide-induced alternative translocation of TM4SF20. The N-terminal sequence of TM4SF20 and the 1st transmembrane helix are highlighted in blue and yellow, respectively. Within the first transmembrane domain, the two polar residues, G22 and N26, are marked by red text. The three N-linked glycosylation sites in loop 3 are indicated. N80 in loop two is not indicated because N80 is not glycosylated due to its close proximity to the transmembrane helix. The A and B forms of TM4SF20 are designated as TM4SF20(A) and TM4SF20(B), and on the left and right panels of the above model, respectively.

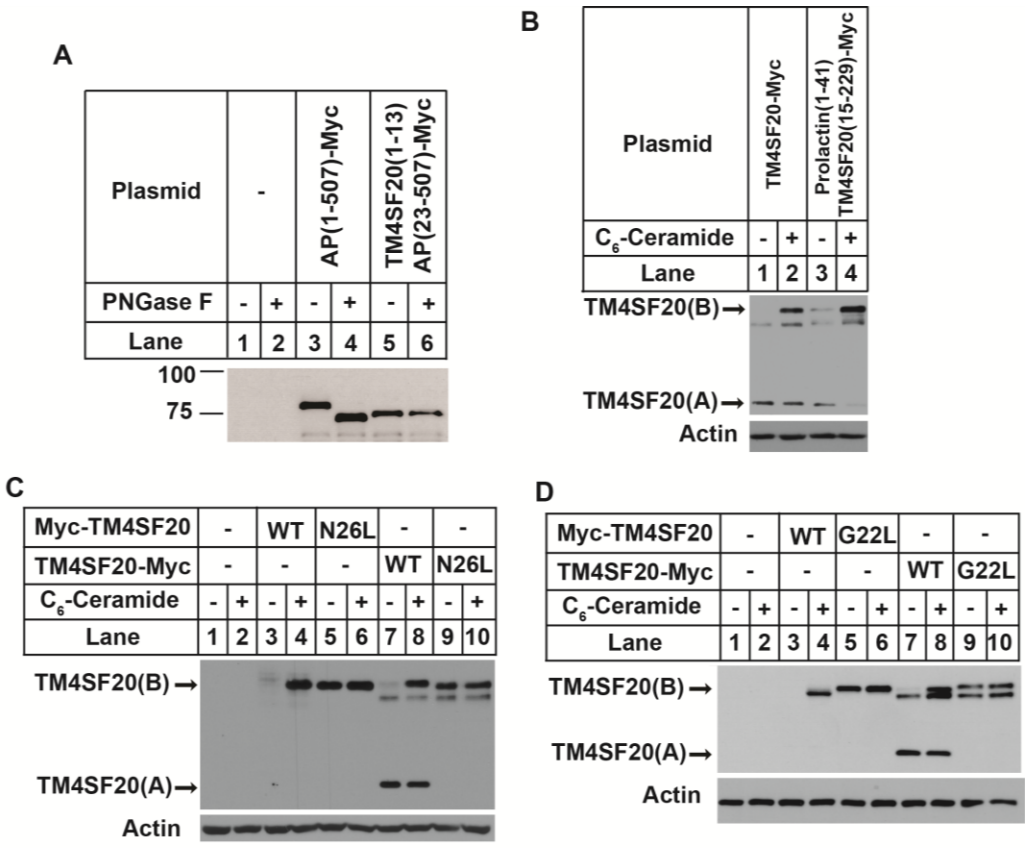

Figure 6. Alternative Translocation of TM4SF20 Depends on the 1st Transmembrane Helix of the Protein

(A) On day 0, A549 cells were seeded at 4×10^5 cells per 60-mm dish. On day 1, cells were transfected with the indicated plasmid, with total DNA adjusted to 2 µg/dish with empty vector. On day 2, cells were treated with or without 6 µM C_6-ceramide for 8 h, after which cells were harvested and the lysates subjected to SDS-PAGE and immunoblot analysis.

(B) A549 cells were seeded, transfected with the indicated plasmid, and treated as described in Figure 7A. After ceramide treatment, cell lysates were incubated with or without PNGase F. Treated cell lysates were then subjected to immunoblot analysis.

(C and D) A549 cells were seeded, transfected with the indicated plasmid, and analyzed as described in Figure 7A.

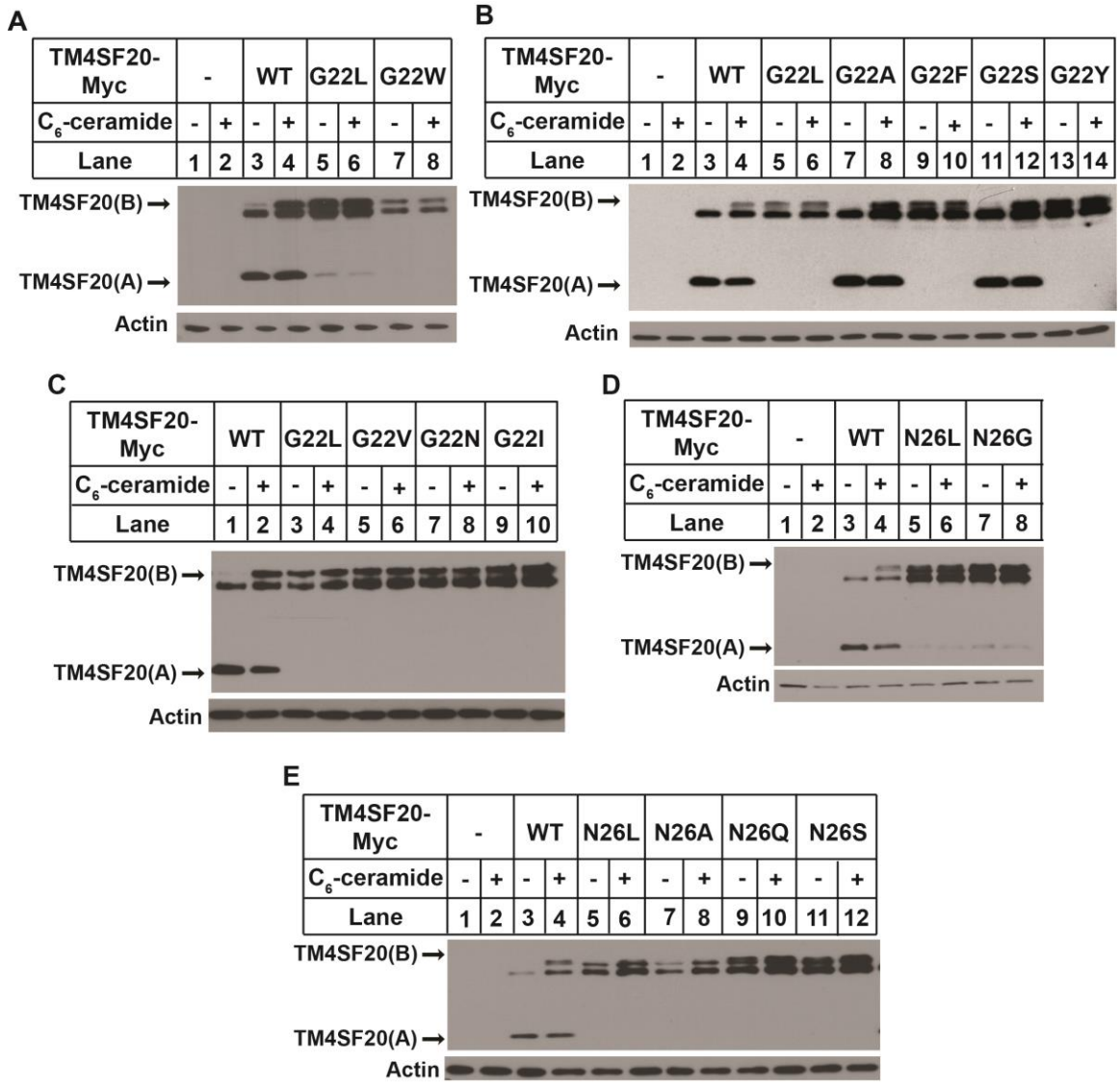

Figure 7. Mutations of Amino Acids G22 and N26 in the 1st Transmembrane Helix of TM4SF20 to Significantly More Hydrophobic Residues Results in TM4SF20(B) Regardless of Ceramide Treatment

(A, B, C, D, E) On day 0, A549 cells were seeded at 4×10^5 cells per 60-mm dish. On day 1, cells were transfected with the indicated plasmid, with total DNA adjusted to 2 μg/dish with empty vector. On day 2, cells were treated with or without 6 μM C_6-ceramide for 8 h, after which cells were harvested and the lysates subjected to SDS-PAGE and immunoblot analysis (A, B, C, and E performed by JungYeon Kim).

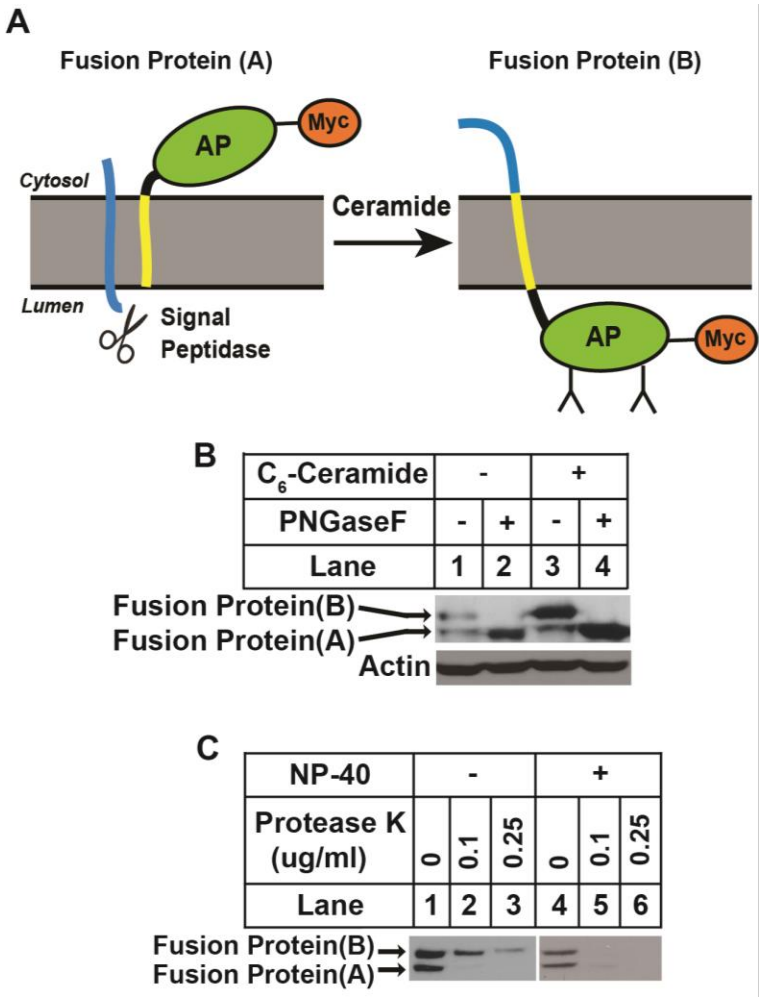

Figure 8. The 1st Transmembrane Helix of TM4SF20 is Sufficient for Alternative Translocation of a Fusion Protein in Response to Ceramide

(A) A model predicting the ceramide-induced alternative translocation of a fusion protein made by C-terminal Myc-tagged AP with its N-terminal signal sequenced replaced by the first 36 amino acid residues of TM4SF20 containing the N-terminal sequence (blue) and the first transmembrane helix (yellow)

(B and C) A549 cells were seeded at 4×10^5 cells per 60-mm dish. On day 1, cells were transfected with 0.5 µg of the plasmid encoding the fusion protein, pTK-TM4SF20(1-36)-AP(18-507)-Myc. On day 2, the cells were treated with 3 µM of C_6-ceramide for 8 h as indicated. (B) cell lysates were subjected to PNGase F treatment as indicated followed by immunoblot analysis with anti-Myc to detect transfected fusion protein. (C) Membrane vesicles of ceramide-treated cells were subjected to protease protection assay as previously described in Figure 2D (Figure 8C performed by Qiuyue Chen).

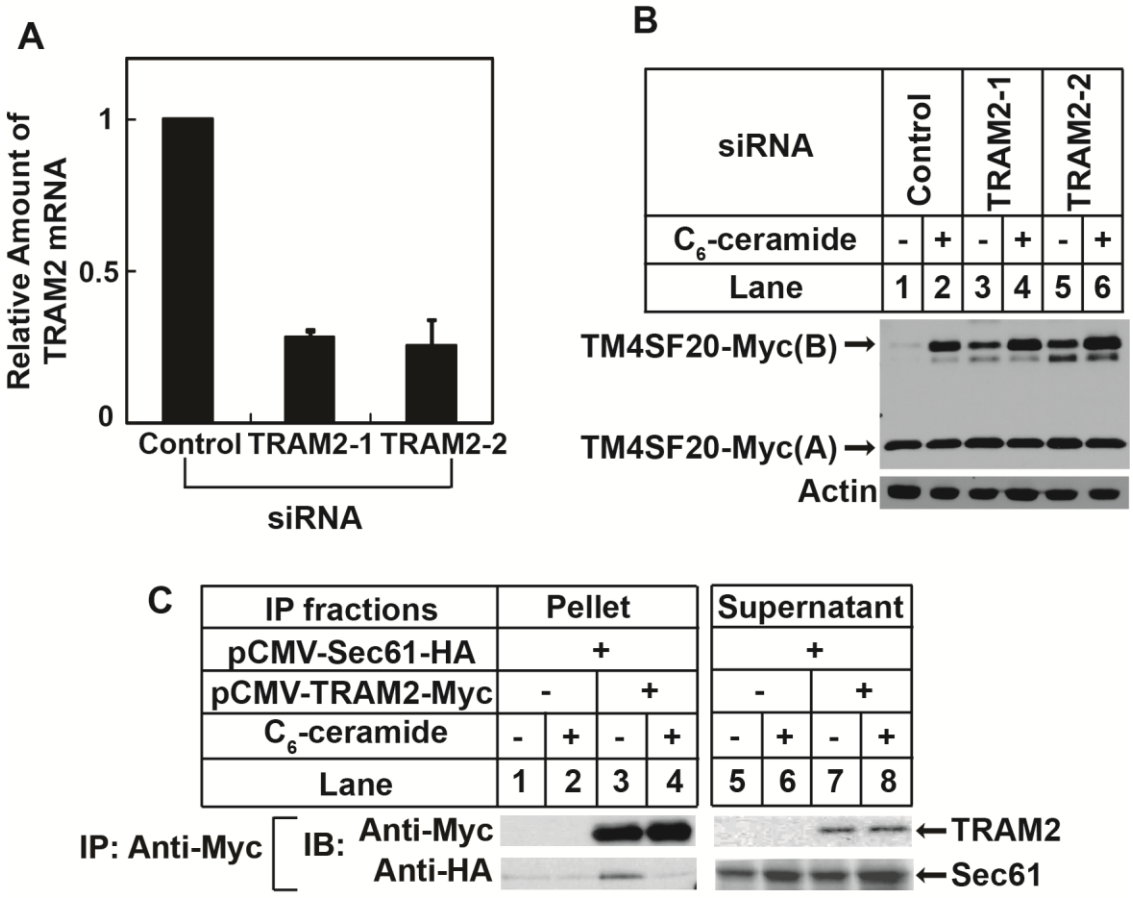

Figure 9. Ceramide Induces Alternative Translocation of TM4SF20 by Triggering the Dissociation of TRAM2 From the ER Translocon

(A and B) On day 0, A549/pTM4SF20 cells were seeded at 1×10^5 cells per 60-mm dish. On day 1, the cells were transfected with the indicated siRNAs. (A) On day 4, some cells were harvested for RNA for quantification of TRAM2 mRNA by RT-QPCR, (B) the remainder of the cells were treated with 6 μM C_6-ceramide for 8 h or left untreated as a control, with cell lysates harvested and subjected to immunoblot analysis with anti-Myc antibody.

(C) On day 0, A549 cells were seeded at 3.5×10^5 cells per 60-mm dish. On day 1, the cells were transfected with 0.15 μg pCMV-TRAM2-Myc and 0.1 μg pCMV-Sec61-HA, with total DNA adjusted to 2 μg/dish with empty vector. On day 2, cells were treated with or without 6 μM C_6-ceramide for 8 h. Transfected TRAM2 was immunoprecipitated as described in Methods. Pellet and supernatant fractions of the immunoprecipitation (loading ratio 1:1) were subjected to immunoblot analysis with the indicated antibodies (experiment performed by Jinyong Kim).

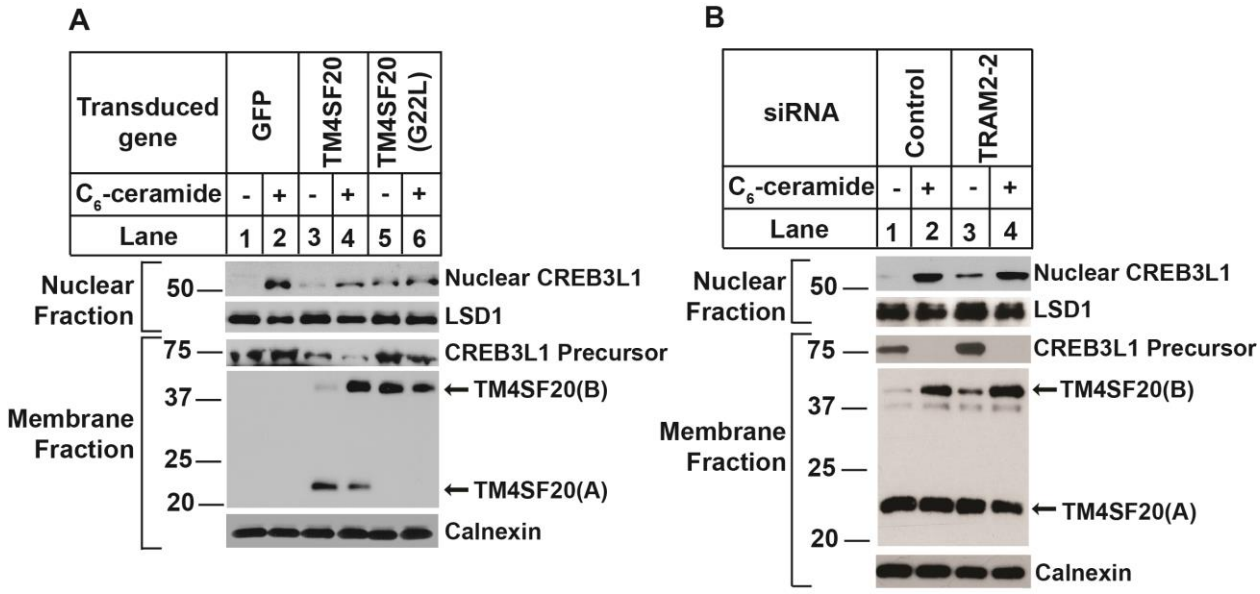

Figure 10. TM4SF20(B) Activates CREB3L1 Cleavage
(A) A549 cells were seeded on day 0 at 1.5×10^6 cells per 100-mm dish. On day 1, cells were infected with lentivirus particles containing plasmids encoding for the indicated proteins. On day 2, 24 h after infection, cells were switched into fresh medium containing 2 µg/ml puromycin for the selection of virus-infected cells. On day 4, cells were treated with or without 6 µM C_6-ceramide for 8 h. Cells were then harvested and analyzed as described in Figure 1C.
(B) A549/pTM4SF20 cells were set up, transfected, and treated as described in Figure 9 A and B. Cells were then fractionated into nucleus and membrane fractions for analysis of CREB3L1 RIP as described in Figure 1C.

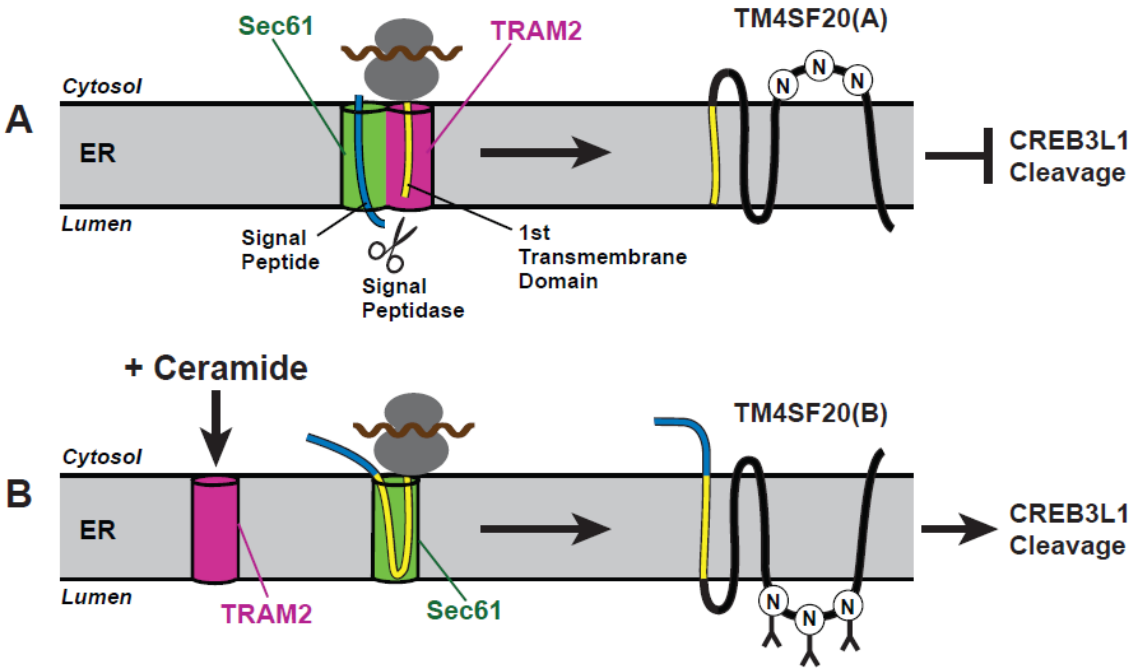

Figure 11. Model Illustrating the Ceramide-Induced Alternative Translocation of TM4SF20

Under normal circumstances, TRAM2, a component of the ER translocon containing Sec61, allows for the N-terminus of TM4SF20 expressed in cells to function as a signal sequence and produce TM4SF20(A), a form of the protein that inhibits CREB3L1 RIP (A). Ceramide presumably interacts with TRAM2, and that in that interaction, dissociates TRAM2 from the ER translocon component Sec61. Following this TRAM2 and Sec61 dissociation, the N-terminus of TM4SF20 can no longer function as a signal peptide, resulting in the production of TM4SF20(B). TM4SF20(B) adopts a membrane topology completely opposite that of TM4SF20(A). TM4SF20(B) is a form of the protein that stimulates CREB3L1 RIP.

CHAPTER THREE
Materials and Methods

Materials

Doxorubicin, sphingomyelinase, N-Hexanoyl-D-sphingosine (C6 -Ceramide), cycloheximide and rabbit anti-actin were obtained from Sigma (St. Louis, MO). We obtained rabbit anti-LSD1 from Cell Signaling (Boston, MA); mouse anti-calnexin from Enzo Life Sciences (Farmingdale, NY). Hybridoma cells producing IgG-9E10, a mouse monoclonal antibody against Myc tag, were obtained from the American Type Culture Collection (Manassas, VA). A rabbit polyclonal antibody against human CREB3L1 was generated as previously described (Denard et al., 2011). A mouse monoclonal antibody against human CREB3L1 (10H1) was previously described (Denard et al., 2015). Peroxidase-conjugated secondary antibodies were from Jackson ImmunoResearch.

Endo H and PNGase F were obtained from New England BioLabs. MG132 and Nonidet P-40 alternative (Nonidet P-40) were from Calbiochem. Methionine, L-[^{35}S]-Stabilized Aqueous Solution, EasyTag was obtained from Perkin Elmer.

X-treme GENE HP was obtained from Roche and used for all A549 transfections as per protocols from the manufacturer. Fugene 6 was obtained from Promega, and used per manufacturer's protocols for transfections to generate lentiviral particles.

Doxorubicin stock solution (2.5 mg/ml) was made by adding nuclease-free water (Ambion) directly to the vial, and stored at 4°C for no more than 1 month. C_6-ceramide

stock solution (15mM) was made by adding DMSO (Sigma) directly to the vial, aliquoted and stored at -80°C, each aliquot is used with only one freeze-thaw.

Cell Culture

A549 cells were maintained in medium A (1:1 mixture of Ham's F12 medium and Dulbecco's modified Eagles' medium containing 100U/ml penicillin, 100 µg/ml streptomycin sulfate, and 5% [vol/vol] fetal calf serum). A549/pTM4SF20 cells were generated by transfecting A549 cells with pCMV-TM4SF20-Myc followed by selection with 700 µg/ml G418. The cells were maintained in medium A supplemented with 700 µg/ml G418. All A549 and A549 stable cell lines were cultured in monolayers at 37°C in 8.8% CO_2. SV589 cells were maintained in medium A (Dulbecco's modified Eagle's medium with 4.5 g/l glucose, 100 U/ml penicillin, 100 µg/ml streptomycin sulfate, and 10% fetal calf serum). SV589 cells were cultured in monolayers at 37°C in 5.0% CO_2.

Plasmids

pCMV-TM4SF20-Myc encodes full length human TM4SF20 followed by 5 tandem repeats of the My epitope tag and 6 histidines. pCMV-Myc-TM4SF20 encodes full length human TM4SF20 with 5 tandem repeats of the Myc epitope tag at the N-terminus. pCMV-SPCS3 encodes full length human SPCS3 with synonymous mutations against siRNA knockdown. pCMV-TRAM2-Myc encodes full length human TRAM2 followed by 5 tandem repeats of the Myc epitope tag and six histidines. pCMV-Sec61-

HA encodes full length human Sec61A1 followed by 3 tandem repeats of the HA epitope tag.

pCMV-prolactin(1-41)-TM4SF20(15-229)-Myc encodes a fusion protein consisting of the N-terminal 41 amino acids of bovine prolactin, two amino acids (LE) encoding the sequence for the restriction enzyme site XhoI, amino acids 15 to 229 of human TM4SF20, and five tandem copies of the Myc epitope followed by six histidines. pCMV- AP(1-507)-Myc encodes amino acids 1 to 507 of human placental alkaline phosphatase (AP) followed by five tandem repeats of the Myc epitope tag and 6 histidines. pCMV-TM4SF20(1-13)-AP(23-507)-Myc encodes a fusion protein consisting of amino acids 1 to 13 of TM4SF20, directly fused to AP from amino acids 23 to 507 followed by five tanem copies of the Myc epitope and six histidines. pTK-TM4SF20(1-36)-AP(18-507)-Myc encodes a fusion protein consisting of amino acids 1 to 36 of TM4SF20, two amino acids (AS) encoding the sequence for the restriction enzyme site NheI, amino acids 18 to 507 of AP, and five tandem copies of the Myc epitope followed by six histidines.

Except for pTK-TM4SF20(1-36)-AP(18-507)-Myc where the expression of the fusion protein is driven by the weak thymidine kinase protein, expression of proteins encoded by the other plasids were driven by the Cytomegalovirus promoter.

pLX-TM4SF20-Myc and pLX-TM4SF20(G22L)-Myc encode the wild type or the glycine 22 to leucine mutation of TM4SF20 followed by five tandem copies of the Myc epitope. The plasmid was generated through an intermediate plasmid based on

pDONOR201 vector, and the final plasmid was generated using the Gateway LR Clonase II (Invitrogen) as per the manufacturer protocols.

Oligonucleotide site-directed mutagenesis was carried out with complementary primers using QuickChange Site-Directed Mutagenesis kit from Stratagene. Oligonucleotide site-directed mutagenesis used to fuse proteins together without restriction enzyme site additions, such as for pCMV-TM4SF20(1-13)-AP(23-507)-Myc was carried out with one single forward, PAGE-purified primer using QuickChange Multi-Site Directed Mutagenesit kit from Stratagene. Open reading frames in all plasmids were confirmed by DNA sequencing. Plasmids were transfected into cells using X-tremeGENE HP (Roche) according to the manufacturer's instructions.

RNA interference

Duplexes of siRNA were synthesized by Dharmacon GE Lifesciences. The siRNA sequence targeting human SPCS3 is UGAUAUAACUGCUGAUCUA. The siRNA sequence targeting human TRAM2 are UGGAAUGAGCAGAGUGCAA and GGCAUUUGAUCCCGAGAAA. The siRNA targeting GFP reported previously (Adams et al., 2004) was used as a control. The scramble sequence AGGAGCAGGAGGAGCUGGA was used as a control siRNA for Figure 10. Cells were transfected with Lipofectamine RNAiMAX (Invitrogen) as described by the manufacturer, after which cells were used to experiments as described in the figure legends.

RT-PCR

RT-PCR was performed as previously described (Liang et al., 2002). In brief, total RNA prepared from cells using the RNeasy mini kit (Qiagen) according to manufacturer's protocols and then treated with RNase-free DNase I (Qiagen). First-strand cDNA was synthesized from 2 µg DNA-free RNA by random hexamer primers and the ABI cDNA synthesis kit (Applied Biosystems). cDNA was mixed with SYBR Green PCR Master Mix (Applied Biosystems) and sets of forward and reverse primers specific for the RNA. The cDNA plus specific primers were analyzed by real-time QPCR with the ABI PRISM 7900HT sequence detection system (Applied Biosystems). All reactions were performed in triplicate. The relative amounts of RNAs were calculated through the comparative cycle threshold method by using human 36B4 mRNA as the invariant control.

Immunoblot

Cells were harvested and separated into nuclear and membrane fractions as previously described (Sakai et al, 1996). The resulting nuclear and membrane fractions were analyzed by SDS-PAGE followed by immunoblot analysis with the indicated antibodies (1:4000 dilution for anti-calnexin, 1:2000 dilution for anti-Myc and rabbit polyclonal anti-CREB3L1, 1:5000 dilution was used for anti-actin). Alternatively, cells were harvested and processed into whole cell lysates by resuspending in buffer A (25mM Tris-HCl pH 7.2, 0.15M NaCl, 1% NP-40, 5µg/ml pepstatin, 10 µg/ml leupeptin, 2 µg/ml aprotinin, 2 µg/ml N-[N-(N-Acetyl-L-leucyl)]-L-norleucine), and rotating at 4°C for 1 h.

After which cells were subject to centrifugation at 20,000 × g for 10 min, the cleared supernatants were then analyzed by SDS-PAGE followed by immunoblot analysis with the indicated antibodies. Bound antibodies were visualized with a peroxidase conjugated secondary antibody using the SuperSignal ECL-HRP substrate system (Thermo Fisher).

Endo H and PNGase F endoglycosidase treatment

Cells were harvested and processed into whole cell lysates by resuspending in buffer A (25mM Tris-HCl pH 7.2, 0.15M NaCl, 1% NP-40) and rotating at 4°C for 1 h. After which cells were subject to centrifugation at 20,000 × g for 10 min, the cleared supernatants were then subjected to the indicated endoglycosidase treatment per the manufacturer's protocols, but with a final increased incubation time at 37°C of 4 h. After which the treated cell lysates were then analyzed by immunoblot.

Vesicle preparation

Intact membrane vesicles were prepared as previously described (Feramisco et al., 2004). Briefly, cell pellets from triplicate dishes were resuspended in 0.4 ml of Buffer A1 (10mM Hepes-KOH (pH 7.4), 10mM KCl, 1.5mM MgCl2,5mM sodium EDTA, 5mM sodium EGTA, and 250mM sucrose), passed through a 22.5-gauge needle 20 times, and centrifuged at 1000×g for 5min at 4˚C. The supernatant centrifuged at 2×104 ×g for 30 min at 4˚C. The pellets were then resuspended in buffer A2 (Buffer A1 containing 100mM NaCl).

Protease K treatment

Protease K treatment was performed as described before with minor modifications (Feramisco et al., 2004): Aliquots of membranes (50µg of proteins) were treated with indicated amount of protease K in the absence or presence of 1% NP-40 in a total volume of 50µl for 1h at 37˚C. After incubation, 12.5µl of laemmli buffer (150mM Tris-HCl (pH 6.8), 15% SDS, 25% glycerol, 0.02% (w/v) bromophenol blue, 12.5% (v/v) 2-mercaptoethanol) was added and samples were boiled for 5min. All the samples were subjected to SDS/PAGE and immunoblot analysis.

Immunoprecipitation

Immunoprecipitation of Myc tagged TM4SF20 was performed with pooled cell pellets from 3 dishes of indicated cells resuspended in 0.4 ml of buffer A (25 mM Tris-HCl pH 7.2, 0.15 M NaCl, 1% Nonidet P-40, 5µg/ml pepstatin, 10 µg/ml leupeptin, 2 µg/ml aprotinin, 2 µg/ml N-[N-(N-Acetyl-L-leucyl)-L-leucyl]-L-norleucine). Cell lysates were rotated at 4 °C for 1 h and clarified by centrifugation at 20,000 × g for 10 min. The lysates were pre-cleared by incubation for 1 h at 4°C with 50 µl of Protein A/G agarose beads (Santa Cruz Biotechnology). The pre-cleared lysates were rotated for 16 h at 4°C with anti-c-Myc agarose beads (Sigma). After centrifugation at 200 × g for 5 min, the resulting supernatants were collected. The pelleted beads were washed for three times with 0.5 ml of buffer A, followed by suspension in 60 µl Laemmli sample buffer dissolved in buffer A. Immunoprecipitated material was eluted by boiling and collected

following centrifugation. Pellet fractions were then subjected to SDS/PAGE, and immunoblot or phosphor screen imaging as appropriate.

Immunoprecipitation of Myc-tagged TRAM2 was carried out with anti-c-myc agarose beads (Sigma) in buffer A (25mM Tris-HCl pH 7.2, 0.15M NaCl, 1% CHAPS, 5µg/ml pepstatin, 10 µg/ml leupeptin, 2 µg/ml aprotinin, 2 µg/ml N-[N-(N-Acetyl-L-leucyl)]-L-norleucine) as previously described (Lee et al., 2008).

Lentivirus infection

cDNA encoding the wild type or mutant TM4SF20-Myc was cloned into the lentiviral vector pLX201, and packaged into lentivirus particles in 293T cells as previously described using Fugene 6 transfection reagent from Promega (Yang et al., 2011). A549 cells were seeded on day 0 at 1.5×10^6 cells per 100-mm dish. On day 1, cells were infected with lentivirus packing plasmids encoding for the indicated proteins. A549 cells were infected with the lentivirus at a multiplicity of infection of 0.8 with 10 µg/ml polybrene. On day 2, 24 h after infection, cells were switched into fresh medium containing 2 µg/ml puromycin for the selection of the virus-infected cels. On day 4, cells were treated with or without 6 µM C_6-ceramide for 8 h. Cells were harvested and separated for the membrane and nuclear fractions as previously described (Sakai et al., 1996).

CHAPTER FOUR
Discussion

The major findings of this current study are summarized in a model presented in Figure 11. The model proposes that in the absence of excess ceramide, TRAM2 is associated with Sec61 in the ER translocation complex. This association of TRAM2 and Sec61 permits the first transmembrane domain to force the N-terminal sequence of the nascent polypeptide chain of TM4SF20 to function like a signal peptide (Figure 3F). The production of TM4SF20 in normal conditions produces TM4SF20(A), which is not glycosylated due to its orientation in the ER membrane. A previous study showed that TM4SF20(A) can function to inhibit the proteolytic activation of CREB3L1 (Chen et al., 2014) . Ceramide accumulation in the ER causes the dissociation of TRAM2 and Sec61 (Figure 6D). When TRAM2 is absent from the ER translocation complex, the N-terminal sequence of the nascent polypeptide chain of TM4SF20 can no longer be cleaved as a signal peptide. This results in the alternative translocation of TM4SF20 seen to produce the glycosylated TM4SF20(B) with a membrane topology completely opposite to that of the A form usually produced. In contrast to the A form that functions to inhibit CREB3L1 cleavage, TM4SF20(B) appears to stimulate CREB3L1 cleavage instead (Figure 10). This mechanism has been termed "alternative translocation."

The alternative translocation of TM4SF20 in response to ceramide results in opposing topologies of the protein produced under different conditions, and this causes TM4SF20 to be modified differently between the two conditions and topologies. Usually, TM4SF20 is produced such that the potential glycosylation sites between the third and fourth transmembrane domains remain in the cytosol. However, when TM4SF20 undergoes ceramide-induced alternative translocation, the potential glycosylation sites between the third and fourth transmembrane is then located in the ER lumen where it can undergo N-linked glycosylation. Alternatively translocated TM4SF20 must also contain additional post-translational modifications as treatment of the protein with the endoglycosidase PNGase F did not completely reduce its apparent molecular weight to that of the unglycosylated TM4SF20. It will be of interest to determine if endogenously expressed TM4SF20 can undergo alternative translocation as well as what other post-translational modifications other than N-linked glycosylation are made to alternatively translocated TM4SF20.

The alternative translocation of TM4SF20 appears to be a regulatory mechanism for the protein. TM4SF20 was identified as a protein which inhibits CREB3L1 RIP (Chen et al., 2014). However, ceramide-induced CREB3L1 RIP is not inhibited by TM4SF20 overexpression (Figure 1C). The overexpression of the alternatively translocated and glycosylated TM4SF20(B) functioned to activate the proteolytic cleavage of CREB3L1 rather than inhibit CREB3L1 RIP (Figure 9). The first transmembrane domain of TM4SF20, rather than the N-terminal sequence, determines the ability of TM4SF20 to alternatively translocate in response to ceramide (Figure 6, 7, 8). The results suggest that

alternative translocation acts as a mechanism by TM4SF20 can be altered to function in opposing roles in the regulation of CREB3L1 RIP depending on the topology assumed by TM4SF20. Further studies on a mutant form of TM4SF20 permanently locked into the A form would strengthen the current model for the opposing functions and topologies of TM4SF20(A) and TM4SF20(B).

The exact mechanism of how TM4SF20 regulates CREB3L1 RIP remains unclear. However, insight can be had from considering the parallels between CREB3L1 and the transcription factor, sterol regulatory element binding proteins (SREBPs), the best-characterized example of RIP. In the case of SREBPs, the proteins Scap and Insig have been identified as key regulatory proteins for SREBP RIP (Brown and Goldstein, 2009; Ye and Debose-Boyd, 2011). Scap binds SREBPs (Sakai et al., 1997), and in the absence of cholesterol, escorts SREBPs from the ER to the Golgi complex where SREBP undergoes cleavage by S1P and S2P proteases. The processing in the Golgi complex releases the N-terminal transcriptional factor domain of SREBP from the membrane, and allows it to go to the nucleus and activate the transcription of genes requires for cholesterol synthesis and uptake (Brown and Goldstein, 2009; Horton et al., 2003; Ye and DeBose-Boyd, 2011). Excessive amounts of cholesterol allows the binding of Insig proteins to Scap and this interaction retains the Scap/SREBPs complex in the ER. The retention of Scap/SREBPs in the ER spatially separates the transcription factor from the Golgi-localized proteases required to active SREBPs through RIP (Brown and Goldstein, 2009; Yang et al., 2002; Ye and DeBose-Boyd, 2011). TM4SF20(A) and TM4SF20(B) may be analogous to Insig proteins and Scap, respectively; and function as a key

regulatory protein for RIP of CREB3L1. Interaction studies for TM4SF20(A) and TM4SF20(B) will be of great interest to clarify the sufficient and necessary protein-protein interactions for CREB3L1 RIP regulation.

While there is no direct biochemical evidence that TRAM2 is the ceramide sensor for the alternative translocation of TM4SF20, it appears probable as the protein contains a TLC domain. The TLC domain is also present in ceramide synthase and is thought to bind ceramide, or ceramide-derived lipids (Winter and Ponting, 2002). The exact species of ceramide that acts as a TRAM2 ligand is also unknown, and the possibility that it is a ceramide metabolite which is the ligand responsible for inactivating TRAM2 cannot be ruled out. However, indirect evidence in the form of sphingolipid and ceramide profile mass spectrometry measurements suggests that it is indeed a species of ceramide that acts as a TRAM2 ligand, as the only lipid measured to increase more than two-fold for all of the treatments that have been shown to cause TM4SF20 alternative translocation and CREB3L1 RIP is ceramide. The best method by which to address the remaining questions concerning TRAM2 would be to measure the direct binding of ceramide to purified TRAM2. Though this would be challenging for several reasons, the first is to determine a method by which TRAM2 can be purified in large amounts for use in biochemical assays, as neither insect cells nor a stable 293S cell line overexpressing TRAM2 have proven to be suitable for TRAM2 purification in the amounts and purity necessary for *in vitro* assays. Even should the protein purification problems be resolved, there would still remain the difficulty of finding a detergent suitable for permitting a protein with multiple transmembrane domains to bind with a hydrophobic ligand.

The novel mechanism of alternative translocation identified in the current study regulates the function of a transmembrane protein by reversing its membrane topology. While the topology of several bacterial membrane proteins have previously been reported to be altered by varying the levels of phosphatidylethanolamine in membranes, the bacterial mechanism appears different from the current mammalian example of alternative translocation in this study. In the bacterial system, reversal of the membrane topology occurs to pre-synthesized proteins, which are altered in response to lipid manipulation (Bogdanov and Dowhan, 2012; Levy, 1996; Von Heijne, 2006). In the mammalian system reported here, the reverse membrane topology occurs to proteins synthesized after the lipid treatment, the proteins synthesized before lipid addition do not reverse in topology. While there are examples of mammalian transmembrane proteins reported to have dual topologies (Dunlop et al., 1995; Sebag and Hinkle, 2009), the underlying mechanisms have yet to be identified. It would be interesting to test whether alternative translocation is also the mechanism for these proteins to acquire different membrane topology.

This study expands the current understanding of the translocation of transmembrane proteins. The N-terminal sequence of TM4SF20 is not predicted to be a signal sequence at all being both shorter, and less hydrophobic than a typical signal sequence (Petersen et al., 2011). Rather, this study found that the first transmembrane immediately following the N-terminal sequence of TM4SF20 is the critical element for ceramide-induced alternative translocation of TM4SF20. It is possible that the first transmembrane helix interacts with TRAM2 through the two polar residues, G22 and

N26, thereby forcing the preceding sequence through the translocon. Importantly, ceramide appears to specifically induce the translocation of TM4SF20 as it did not affect the function of the signal sequences of NPC1 or Grp94 (data not shown). Replacing the TM4SF20 N-terminal sequence with a prolactin sequence also did not affect the ability of the fusion protein to be alternatively translocated as the first transmembrane helix was left intact. These results suggest that the function of the signal sequences of NPC1 and Grp94 do not depend on TRAM proteins, and that the first transmembrane helix of TM4SF20 is sufficient for alternative translocation. All three of the TRAM proteins, TRAM1, TRAM1L1, and TRAM2, contain a TLC domain (Winter and Ponting, 2002). This makes it possible that ceramide is a global regulator of the alternative translocation of transmembrane proteins through TRAM proteins.

The alternative translocation mechanism is not specific to the A549 cell line, the transient transfection of TM4SF20 into other cell culture lines also demonstrated ceramide-induced alternative translocation. That TM4SF20 was only detected in A549 in the panel of cell culture lines available to our laboratory may be due to problems inherent in testing immortalized cell lines rather than a requirement for TM4SF20 expression in human lung epithelial cells. In regards to other tissues, it will be of interest to test brain tissues for TM4SF20. It has been reported that a deletion of exon 3 eliminates transmembrane domains 3 and 4, and that this exon 3 deletion is associated with delayed language development and white matter hyperintensities in brain imaging (Wiszniewski et al., 2013). The association of TM4SF20 exon 3 deletion with a neurological phenotype suggests that experiments in model organisms may be necessary in the future.

While TM4SF20 is the first mammalian protein observed to undergo alternative translocation, it is likely that it is not the only transmembrane protein that undergoes this type of regulation. Any one of the three TRAM proteins, namely TRAM1, TRAM1L1, and TRAM2, may facilitate the usage of the first transmembrane helices to determine the orientation of other membrane-bound proteins. Remarkably, all three TRAM proteins contain a TLC domain, making it possible for ceramide to be global regulator of alternative translocation. Thus, identification of other proteins subjected to ceramide-regulated alternative translocation will provide new insight into the mechanism through which ceramide affects cell physiology. TM4SF20 is only one of twenty total proteins in the transmembrane 4 L6 superfamily, which are generally not well-characterized, and as such it would be interesting to test if any other members of the family also undergo alternative translocation.

BIBLIOGRAPHY

Adams, C.M., Reitz, J., De Brabander, J.K., Feramisco, J.D., Li, L., Brown, M.S., and Goldstein, J.L. (2004). Cholesterol and 25-hydroxycholesterol inhibit activation of SREBPs by different mechanisms, both involving SCAP and Insigs. J Biol Chem 279, 52772-52780.

Breitling, J., and Aebi, M. (2013). N-linked protein glycosylation in the endoplasmic reticulum. Cold Spring Harb Perspect Biol *5*, 10.1101/cshperspect.a013359.

Bogdanov, M., and Dowhan, W. (2012). LIpid-dependent generation of dual topology for a membrane protein. J Biol Chem *287*, 37939-37948.

Brown, M.S., and Goldstein, J.L. (2009). Cholesterol feedback: from Schoenheimer's bottle to Scap's MELADL. J Lipid Res 50 Suppl, S15-27.

Chen Q., Lee C.-E., Denard B., Ye J. (2014) Sustained Induction of Collagen Synthesis by TGF-β Requires Regulated Intramembrane Proteolysis of CREB3L1. PLoS ONE 9(10): e108528. doi:10.1371/journal.pone.0108528

Choo K. H., and Ranganathan, S. (2008). Flanking singal and mature peptide residues influence signal peptide cleavage. BMC Bioinformatics *9*, S15.

Denard, B., Seemann, J., Chen, Q., Gay, A., Huang, H., Chen, Y., and Ye, J. (2011). The membrane-bound transcription factor CREB3L1 is activated in response to virus infection to inhibit proliferation of virus-infected cells. Cell Host Microbe 10, 65-74.

Denard, B., Lee, C., and Ye, J. (2012). Doxorubicin blocks proliferation of cancer cells through proteolytic activation of CREB3L1. Elife 1, e00090.

Denard, B., Pavia-Jimenez, A., Chen, W., Williams, N. S., Naina, H., Collins, R., Brugarolas, S., Ye, J. (2015). Identification of CREB3L1 as a Biomarker Predicting Doxorubicin Treatment Outcome. *PLoS ONE*, *10*(6), e0129233.

Dunlop, J., Jones, P.C., and Finbow, M.E. (1995). Membrane insertion and assembly of ductin: a polytopic channel with dual orientations. EMBO J *14*, 3609-3616.

Feramisco, J.D., Goldstein, J.L., and Brown, M.S. (2004). Membrane topology of human insig-1, a protein regulator of lipid synthesis. J Biol Chem 279, 8487-8496.

Görlich, D., Hartmann, E., Prehn, S., and Rapoport, T.A. (1992). A protein of the endoplasmic reticulum involved early in polypeptide translocation. Nature *357*, 47-52.

Görlich, D., and Rapoport, T.A. (1993). Protein translocation into proteoliposomes reconstituted from purified components of the endoplasmic reticulum membrane. Cell *75*, 615-630.

Hannun, Y.A., and Obeid, L.M. (2008). Principles of bioactive lipid signalling: lessons from sphingolipids. Nat Rev Mol Cell Biol 9, 139-150.

Hegde, R.S., and Kanb, S.-W. (2008). The concept of translocational regulation. J Cell Biol *182*, 225-232.

Hegde, R.S., and Lingappa V.R. (1997). Membrane protein biogenesis: Regulated complexity at the Endoplasmic Reticulum. Cell *91*, 575-582.

Honma, Y., Kanazawa, K., Mori, T., Tanno, Y., Tojo, M., Kiyosawa, H., Takeda, J., Nikaido, T., Tsukamoto, T., Yokoya, S., et al. (1999). Identification of a novel gene, OASIS, which encodes for a putative CREB/ATF family transcription factor in the long-term cultured astrocytes and gliotic tissue. Brain Res Mol Brain Res 69, 93-103.

Horton, J.D., Shah, N.A., Warrington, J.A., Anderson, N.N., Park, S.W., Brown, M.S., and Goldstein, J.L. (2003). Combined analysis of oligonucleotide microarray data from transgenic and knockout mice identifies direct SREBP target genes. Proc Natl Acad Sci U S A 100, 12027-12032.

Hua, X., Sakai, J., Brown, M.S., and Goldstein, J.L. (1996). Regulated cleavage of sterol regulatory element binding proteins requires sequences on both sides of the endoplasmic reticulum membrane. J Biol Chem 271, 10379-10384.

Kitatani, K., Idkowiak-Baldys, J., and Hannun, Y.A. (2008). The sphingolipid salvage pathway in ceramide metabolism and signaling. Cell Signal *20*, 1010-1018.

Kyte, J., and Doolittle, R.F. (1982). A simple method for displaying the hydropathic character of a protein. J Mol Biol 157, 105-132.

Lee, J.N., Zhang, X., Feramisco, J.D., Gong, Y., and Ye, J. (2008). Unsaturated fatty acids inhibit proteasomal degradation of Insig-1 at a postubiquitination step. J Biol Chem 283, 33772-33783.

Liang, G., Yang, J., Horton, J.D., Hammer, R.E., Goldstein, J.L., and Brown, M.S. (2002). Diminished hepatic response to fasting/refeeding and liver X receptor agonists in mice with selective deficiency of sterol regulatory element-binding protein-1c. J Biol Chem 277, 9520-9528.

Levy, D. (1996). Membrane proteins which exhibit multiple topological orientations. Essay Biochem *31*, 49-60.

Meyer, H.-A., and Hartmann, E. (1997). The yeast SPCC22/23 homolog Spc3p is essential for signal peptidase activity. J Biol Chem *272*, 13159-13164.

Morad, S.A., and Cabot, M.C. (2013). Ceramide-orchestrated signalling in cancer cells. Nat Rev Cancer 13, 51-65.

Murakami, T., Kondo, S., Ogata, M., Kanemoto, S., Saito, A., Wanaka, A., and Imaizumi, K. (2006). Cleavage of the membrane-bound transcription factor OASIS in response to endoplasmic reticulum stress. J Neurochem 96, 1090-1100.

Murakami, T., Saito, A., Hino, S., Kondo, S., Kanemoto, S., Chihara, K., Sekiya, H., Tsumagari, K., Ochiai, K., Yoshinaga, K., et al. (2009). Signalling mediated by the endoplasmic reticulum stress transducer OASIS is involved in bone formation. Nat Cell Biol 11, 1205-1211.

Nikaido, T., Yokoya, S., Mori, T., Hagino, S., Iseki, K., Zhang, Y., Takeuchi, M., Takaki, H., Kikuchi, S., and Wanaka, A. (2001). Expression of the novel transcription factor OASIS, which belongs to the CREB/ATF family, in mouse embryo with special reference to bone development. Histochem Cell Biol 116, 141-148.

Nilsson I.M., and Von Heijne, G. (1992). A signal peptide with a proline next to the cleavage site inhibits leader peptidase when preent in a sec-independent protein. FEBS Lett *299*, 243-246.

Nilsson, I.M., and von Heijne, G. (1993). Determination of the distance between the oligosaccharyltransferase active site and the endoplasmic reticulum membrane. J Biol Chem *268*, 5798-5801.

Omori, Y., Imai, J., Suzuki, Y., Watanabe, S., Tanigami, A., and Sugano, S. (2002). OASIS is a transcriptional activator of CREB/ATF family with a transmembrane domain. Biochem Biophys Res Commun 293, 470-477.

Petersen, T.N., Brunak, S., von Heijne, G., and Neilsen, H. (2011). SignalP 4.0: discriminating signal peptides from transmembrane regions. Nat Meth *8*, 785-786.

Sakai, J., Duncan, E.A., Rawson, R.B., Hua, X., Brown, M.S., and Goldstein, J.L. (1996). Sterol- regulated release of SREBP-2 from cell membranes requires two sequential cleavages, one within a transmembrane segment. Cell 85, 1037-1046.

Sakai, J., Nohturfft, A., Cheng, D., Ho, Y.K., Brown, M.S., and Goldstein, J.L. (1997). Identification of complexes between the COOH-terminal domains of sterol regulatory element- binding proteins (SREBPs) and SREBP cleavage-activating protein. J Biol Chem 272, 20213- 20221.

Sakai, J., Rawson, R.B., Espenshade, P.J., Cheng, D., Seegmiller, A.C., Goldstein, J.L., and Brown, M.S. (1998). Molecular identification of the sterol-regulated luminal protease that cleaves SREBPs and controls lipid composition of animal cells. Mol Cell 2, 505-514.

Sebag, J.A., and Hinkle P.M., (2009). Regions of melanocortin 2 (MC2) receptor accessory protein necessary for dual topology and MC2 receptor trafficking and signaling. J Biol Chem *284*, 610-618.

Shao, S., and Hegde, R.S. (2011). Membrane protein insertion at the endoplasmic reticulum. Annu Rev Cell Dev Biol 27, 25-56.

Shen, J., Chen, X., Hendershot, L., and Prywes, R. (2002). ER stress regulation of ATF6 localization by dissociation of BiP/GRP78 binding and unmasking of Golgi localization signals. Dev Cell 3, 99-111.

Verrecchia, F., and Mauviel, A. (2007). Transforming growth factor-beta and fibrosis. World J Gastroenterol 13, 3056-3062.

Voigt, S., Jungnickel, B., Harmann, E., and Rapoport, T.A. (1996). Signal sequence-dependent function of the TRAM protein during early phases of protein transport across the endoplasmic reticulum membrane. J Cell Biol *134*, 25-35.

Von Heijne, G. (2006). Membrane-protein topology. Nat Rev Mol Cell Biol *7*, 909-918.

Winter, E., and Ponting, C.P. (2002). TRAM, LAG1 and CLN8: members of a novel family of lipid-sensing domains? Trends Biochem Sci 27, 381-383.

Wiszniewski, W., et al. (2013). *TM4SF20* Ancestral Deletion and Susceptibility to a Pediatric Disorder of Early Language Delay and Cerebral White Matter Hyperintensities. *American Journal of Human Genetics*, *93*(2), 197–210.

Wright, M.D., Ni, J., and Rudy, G.B. (2000). The L6 membrane proteins--a new four-transmembrane superfamily. Protein Sci 9, 1594-1600.

Yang, T., Espenshde, P.J., Wright, M.E., Yabe, D., Gong, Y., Aebersold, T., Goldstein, J.L., and Brown, M.S. (2002). Crucial Step in Cholesterol Homeostasis: Sterols Promote Binding of SCAP to INSIG-1, a Membrane Protein that Facilitates Retention of SREBPs in ER. Cell *110,* 489-500.

Ye, J., Dave, U.P., Grishin, N.V., Goldstein, J.L., and Brown, M.S. (2000a). Asparagine-proline sequence within membrane-spanning segment of SREBP triggers intramembrane cleavage by site-2 protease. Proc Natl Acad Sci U S A 97, 5123-5128.

Ye, J., Rawson, R.B., Komuro, R., Chen, X., Dave, U.P., Prywes, R., Brown, M.S., and Goldstein, J.L. (2000b). ER stress induces cleavage of membrane-bound ATF6 by the same proteases that process SREBPs. Mol Cell 6, 1355-1364.

Ye, J., and DeBose-Boyd, R.A. (2011). Regulation of cholesterol and fatty acid synthesis. Cold Spring Harb Perspect Biol 3.

Zimmerman, R., Eyrisch, S., Ahman, M., and Helms, V. (2011). Protein translocation across the ER membrane. Biochim Biophys Acta *1808*, 912-924.